



HAL
open science

Fluvial System Dynamics of Sudano-Sahelian Zone during the Late Holocene. The Yamé River (Dogon Country, Mali)

Aline Garnier, Laurent Lespez

► **To cite this version:**

Aline Garnier, Laurent Lespez. Fluvial System Dynamics of Sudano-Sahelian Zone during the Late Holocene. The Yamé River (Dogon Country, Mali). *Geomorphology*, 2019, 340, pp.32–52. 10.1016/j.geomorph.2019.04.018 . hal-02477281

HAL Id: hal-02477281

<https://hal.science/hal-02477281v1>

Submitted on 22 Oct 2021

HAL is a multi-disciplinary open access archive for the deposit and dissemination of scientific research documents, whether they are published or not. The documents may come from teaching and research institutions in France or abroad, or from public or private research centers.

L'archive ouverte pluridisciplinaire **HAL**, est destinée au dépôt et à la diffusion de documents scientifiques de niveau recherche, publiés ou non, émanant des établissements d'enseignement et de recherche français ou étrangers, des laboratoires publics ou privés.



Distributed under a Creative Commons Attribution - NonCommercial 4.0 International License

1 **Fluvial system dynamics of Sudano-Sahelian zone during** 2 **the Late Holocene. The Yamé River (Dogon Country, Mali)**

3 Aline Garnier^{1*}; Laurent Lespez¹

4 ¹ LGP UMR 8591 CNRS, Département de Géographie, Université de Paris Est-
5 Créteil, 61 avenue du Général De Gaulle, 94010 Créteil, France. e-mail:
6 aline.garnier@lgp.cnrs.fr; laurent.lespez@lgp.cnrs.fr

7 *Corresponding author

8

9 **Abstract**

10 In West Africa, most palaeoenvironmental studies have focused on the role of climatic
11 change on the environment. Because of the richness of its deposits, the Yamé River (Mali), a
12 tributary of the Niger River, offers an opportunity to reconstruct the evolution of this fluvial
13 system in comparison with both climatic and anthropogenic changes during the Late
14 Holocene. To investigate more closely the spatio-temporal response of the fluvial system,
15 sedimentary analyses were conducted on seven reaches distributed along the 137 km length
16 of the Yamé valley. This approach testifies of the possibility for each time slice and river
17 reach (1) to reconstruct the fluvial style and processes and (2) to estimate the sediment
18 storage volume reflecting sediment distribution patterns. Results reveal a wide variability of
19 the sedimentary cascade suggesting contrasting responses to external and local controls.
20 Humid (4200-2900 cal. BP ; 450-24 cal. BP) or arid (2350-1700 cal. BP) phases have been
21 recorded in fluvial archives while an intensification in erosion and sediment supplies, even
22 during the arid period (2900-2350 cal. BP and the 20th century), may be associated with an
23 increase in human pressure. Two other periods are related to both climate and

24 anthropogenic factors. During 1700-1400 cal. BP phase huge sediment supplies can be
25 explained mainly by the reactivation of both hydrological processes and human occupation
26 after an intense and long arid event. Dispersed sediment sinks recorded during the 450-24
27 cal. BP period originate from the combination of intensification of colluvial processes and a
28 wet phase context originating from global climatic change. Thus, this study provides
29 evidence that climate is the strongest driver for the fluvial response of these semi-arid and
30 tropical rivers while human disturbance appear as a secondary factor due to the high
31 sensitivity of the environment to climate variability in such areas.

1. Introduction

Because rivers are highly sensitive to environmental change, fluvial records are widely considered as a good indicator from which to reconstruct past landscapes. Global climatic and anthropogenic changes are considered as the strongest drivers of water discharge and sediment supply fluctuations on which fluvial system depends. However, local controls such as geological settings, geomorphological heritage, vegetation and land use are also relevant in determining fluvial system changes. A fluvial systems response to these forcing factors is extremely complex with considerable spatio-temporal variability (e.g. [Knox, 1983](#); [Notebaert and Verstraeten, 2010](#)).

In West Africa, studies on Holocene fluvial system changes are rare and unevenly distributed across this geographical area and time period. Most of the studies have been conducted between latitudes 16°N and 22°N (Saharan and Sahelian zones) and have focused on the Early and Middle Holocene periods (11500 - 4200 BP). This focus can be explained by the orientation of research conducted in Africa during the last decades which have been mainly aimed at characterizing the spatial and temporal extension of the African humid Period ending around 5000 years ago ([de Menocal et al., 2000](#); [Hely et al., 2009](#); [Lézine et al., 2011](#); [Armitage et al., 2015](#); [Shanahan et al., 2015](#)). Thus, most of the previous fluvial studies have highlighted the role of climatic changes ([Makaske, 1998](#); [Makaske et al., 2007](#); [Gumnior and Thiemeyer, 2003](#); [Gumnior, 2008](#); [Lespez et al., 2011](#)). Only few studies were interested on the last three millennia and the question of the increasing human impact on the landscapes (e.g. the development of agricultural practices, extraction of raw materials for metallurgy and associated wood exploitation etc.; [Garnier et al. 2018](#)). Other palaeoenvironmental studies have mainly focused on lacustrine environments ([Lézine et al., 2011](#); [Shanahan et al., 2006, 2015](#)) or marine cores taken from the mouths of the bigger rivers of West Africa such as the Niger River ([Lézine et al., 2005](#); [Collins et al., 2017](#)) or the Sénégal River ([Bouimetarhan et al., 2009](#); [Niedermeyer et al., 2010](#)). These lacunae in the literature stress the necessity of carrying out new high-resolution investigations into other

28 deposition environments, such as fluvial environments, and more specifically focused on the
29 Late Holocene period.

30 These were the objectives of this study conducted on the sedimentary records of the
31 Yamé River, a tributary of the Niger River. Its catchment area, covering 4400 km², provided a
32 diversity range of landscape units, geomorphological settings, fluvial styles and land use
33 patterns (Garnier et al., 2014). Moreover, because of the exceptional preservation of the
34 fluvial deposits including archaeological remains, the Ounjougou's reach, located in the
35 upper Yamé valley, has already been subject to several palaeoenvironmental and
36 archaeological studies (Huysecom, 2002; Huysecom et al., 2004, 2009; Mayor et al., 2005;
37 Rasse et al., 2006; Lespez et al., 2008, 2011; Ozainne et al., 2009; Le Drézen et al., 2010;
38 Garnier et al., 2013, 2015; Eichhorn and Neumann, 2013). A publication by Lespez et al.
39 (2011) proposed a synthesis of fluvial changes during the Holocene of the Ounjougou's
40 reach and discussed the role of climatic and anthropogenic controls. This study provide
41 information about the local fluvial metamorphosis and the upper catchment landscapes
42 changes. But, a multi-scale approach is necessary to understand the sedimentary responses
43 of this type of medium-scale river basin. The study of six new reaches in the lower valley
44 allows for the characterization of the general pattern of sedimentary dynamics and the
45 longitudinal complexities of the alluvial filling during the Holocene. A particular focus of this
46 research was on the internal arrangement of the catchment area and the flow connectivity at
47 different spatio-temporal scales. In addition, estimation of the sediment storage for each
48 reach provides information about the sediment delivery and the sedimentary cascade. From
49 the onset of the Late Holocene onwards (4200-0 cal. BP), the Yamé fluvial system witnessed
50 a wide variability of sedimentary cascade suggesting a contrasting response to external and
51 local controls. A comparison of our data with those from other regional and local
52 palaeoenvironmental studies allows for the examination and discussion of the role of each
53 forcing factor in the geomorphological adjustment of the Yamé catchment area.

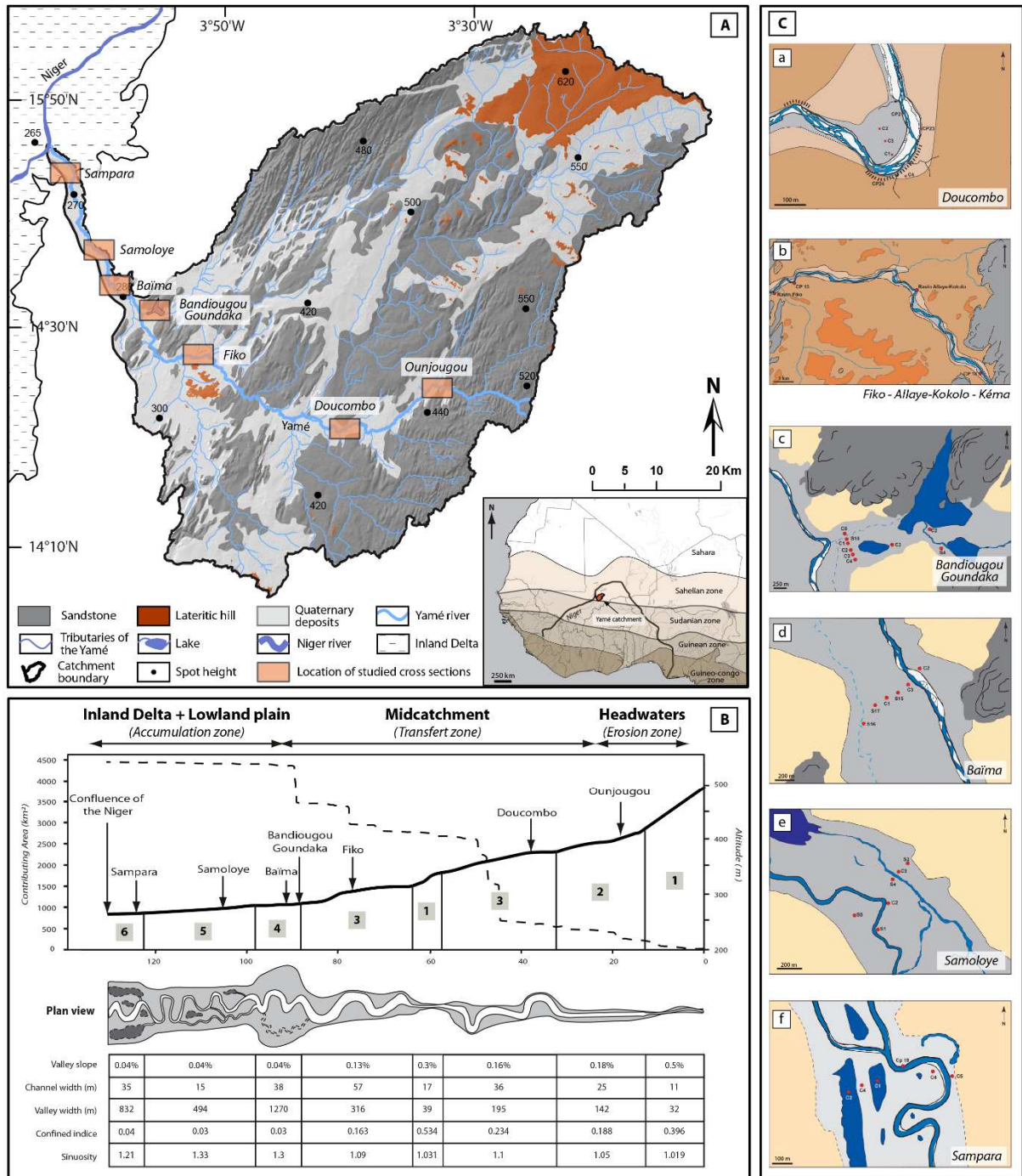
54 **2. Study area and previous work**

55 **2.1. Study area**

56 The Yamé River, a right-bank tributary of the Niger River, is the main stream of the
57 Dogon Country (Mali) in the Sudano-Sahelian zone (Fig.1). Being 137 km long, from east to
58 west, the longitudinal profile of the valley bottom is complex. Based upon classical
59 morphological data (slope, channel / valley width, confined indice, sinuosity; Fig.1B), six river
60 styles were identified and displayed a range of features and behaviors from confined valley
61 to laterally unconfined valley settings (Garnier et al., 2014). These six river styles are
62 displayed into four different river units: the headwater, midcatchment, lowland plain and
63 inland delta domains (Fig.1). After crossing the sandstone plateau in the upper valley (500
64 m), on which remain many lateritic hills, the Yamé River flows in the midcatchment across
65 the Pleistocene deposits resulting from the reworking of aeolian silts deposited during the
66 last dry period (Rasse et al., 2006). The lower valley is characterized by a large glaciais,
67 common to the Sahelian zone, in which the Yamé River is slightly incised. Downstream, the
68 Yamé flows at 267 m towards the Niger River in the Inland Delta.

69 The discharge regime of the Yamé is characterized by great spatial and temporal
70 variability reflecting (1) the seasonal rainfall regime of the Sudano-Sahelian belt and (2) the
71 local geological features. In the headwaters, until the Ounjougou's reach, the sandstone
72 aquifers feed the river and enable low flow during the dry season (October to June).
73 Otherwise, in the middle and lower valley the Yamé River dries up from the month of January
74 onwards. The three month long rainy season (July to September), associated with the
75 northward displacement of the monsoon, occurs as an intense rainstorm and generates all
76 along the valley flood flows with a high velocity and channel avulsion within the valley
77 bottom. Due to the orographic effect, regional rainfall amount is greatest on the sandstone
78 plateau (563 mm/yr) and less in the Inland Niger Delta (520 mm/yr). As a result of this spatial
79 and temporal discharge, the valley floor vegetation appears different upstream and
80 downstream. Upstream, on the sandstone plateau, intense gardening by human groups
81 occurs all year long thanks to the presence of water. Downstream, in the Inland Delta, the

82 important water discharge and the slower receding waters of the Niger during the rainy
 83 season allow for rice cultivation. Otherwise, the whole catchment area is today covered by
 84 agricultural fields, mainly growing pearl millet (*Pennisetum glaucum*) and a Sahelo-Sudanian
 85 savanna strongly altered by humans (Eichhorn and Neumann, 2013).



86

87

Fig. 1: Geomorphological map of the Yamé valley

88 **A. Geomorphological map of the Yamé catchment; B. Description of the six River style**
89 (highlighted in grey) (1) The bedrock-controlled occasional floodplains River Style (2) The low
90 sinuosity planform-controlled River style (3) The meandering irregular planform-controlled
91 discontinuous floodplain River Style (4) Meandering channel in an extensive continuous floodplain (5)
92 The multiple meandering channels (6) Meandering Rivers in a swampy floodplain associated to the
93 Inland Niger Delta ; **C. Planform on the studied reaches and location of investigations** (a-b) River
94 Style n°3; (c-d) River Style n°4; (e) River Style n°5; (f) River Style n°6.

95

96 **2.2. Previous work**

97 The previous research has focused on the Ounjougou reach situated 18 km from the
98 spring of the river. The sedimentary succession is exceptionally long and has yielded
99 archaeological materials from the Middle Palaeolithic to modern times (Huysecom et al.,
100 2004). The geomorphological setting has been described in previous publications (Rasse et
101 al., 2004, 2006 ; Lespez et al., 2008) and a final synthesis of the fluvial system changes
102 published (Lespez et al., 2011). Thus, this reach represents a reference site for the fluvial
103 system response to environmental changes in West Africa. Moreover, palaeobiological data,
104 e.g. phytoliths, pollen and charcoal analyses, yielded additional information about the
105 Holocene environmental changes for the Ounjougou's site (Neumann et al., 2009; Le Drézen
106 et al., 2010, 2014; Eichhorn et al., 2010; Eichhorn and Neumann, 2013; Garnier et al., 2013).
107 During the Late Holocene four major periods of fluvial change have been highlighted. At the
108 beginning (4200-2350 cal BP), the sedimentation indicates a seasonal pattern with a drying
109 up of the floodplain with active flood channels and drying up of ponds. This scenario is
110 corroborated by the vegetation records with a disappearance of some Sudano-Guinean taxa
111 and the gradual appearance of Sudano-Sahelian species (Eichhorn and Neumann, 2013).
112 Locally, we observed on the surrounding plateau areas the development of colluvial deposits
113 as recovered during the archaeological excavation (Ozainne et al., 2009). Later, between
114 2350 and 1700 cal. BP, a sedimentary hiatus and a deep incision in the earlier deposits was
115 observed (Garnier et al., 2015). It can be interpreted as the result of the high-energy flood

116 flows that occurred during a dry period. Then, the last two millennia were characterized by
117 large variability of river dynamics reflecting a contrasted climatic period. Thus, there was an
118 oscillation between a rhythmic sedimentation rate characterized by slow flows (1630-1410
119 and 930-690 cal. BP) alternates with periods of active flows (1320-910 and 700-450 cal. BP).
120 Meanwhile, there was a widespread accumulation of colluvium over the past two millennia
121 over the entire stretch of the Ounjougou, filling the valley floor. These thick colluvial deposits,
122 reaching 4m locally, generated the formation of a sedimentary plug and forced the
123 repositioning of the River path over the course of the four centuries. Finally, between 450-24
124 cal. BP a new metamorphosis occurred with the development of a large wetland in the valley
125 bottom.

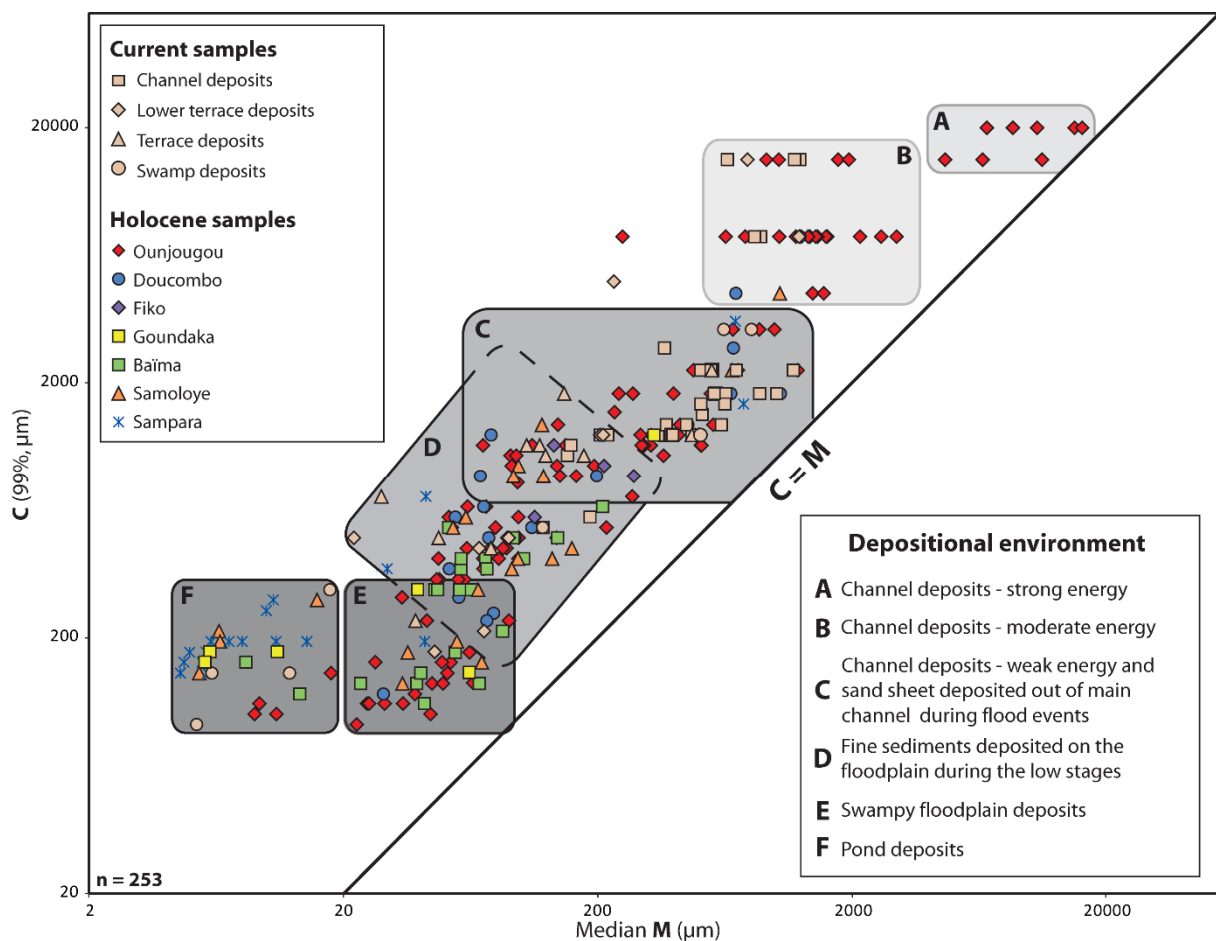
126 **3. Materials and methods**

127 In order to investigate the entire fluvial system, new geomorphological investigations were
128 undertaken along the Yamé valley. The first step was to identify homogeneous landscapes
129 units and hydro-geomorphological processes. Thus, the valley floor and channel surface
130 areas were digitalized for the entire valley and split into 500m long sections (see [Garnier et](#)
131 [al., 2014](#)). Then, for each 500m section, five classical morphological indices have been
132 calculated (channel and valley floor width, confined indices, sinuosity and secondary channel
133 area). Discontinuities within the longitudinal series of geomorphological parameters were
134 identified by a Pettitt rupture test (Pettitt, 1979). This methodology allowed to dissociate eight
135 different sections grouping elementary segments with similar morphological characteristics
136 and six river styles (Garnier et al., 2014). Except in the bedrock-controlled occasional
137 floodplains River Style (N° 1; Fig.1) where alluvial deposits are absent or very current,
138 investigations were conducted in each River Style. From upstream to downstream, seven
139 cross sections were surveyed by laser range meter while the architecture of alluvial filling
140 was established through , thirty-two outcrop profiles (1-4m deep), fourteen hand augers (4-
141 6m deep) and twenty-two boreholes (4-10m deep). Boreholes have been recovered along
142 the cross-sections with a portable Cobra vibracorer using a 1m long steel drill-pipe.

143 **3.1. Granulometry**

144 Eighty-nine sediment samples from all lithofacies of the different sections were analyzed
 145 and compared with sixty modern samples from the valley floor (Fig. 2).

146 Granulometry was measured by laser particle analyser (Coulter Counter LS 200), adjusted
 147 for measurements from the ≤ 2 mm fraction. Coarse material was removed and grain-size
 148 was determined using a series of sieves ranging from 2 to 5 mm. In particular, the C-M
 149 pattern (Passega, 1957, 1964; Bravard and Peiry, 1999) in which C is the one-percentile and
 150 M the median of the grain size distribution, was used to distinguish the depositional
 151 environments by the criteria of competence and mode of sediment transport. Including the
 152 previously studied Ounjougou's samples (Lespez et al., 2011), a C-M diagram of 253
 153 samples from the whole Yamé valley was constructed and allowed for the identification of six
 154 depositional environments (Fig. 2).



155

156 **Fig. 2: C-M diagram of Holocene and modern alluvial deposits of the Yamé**
157 **valley**

158

159 **3.2. Facies identification**

160 The approach used in this study is based on an accurate classification of the sedimentary
161 facies for the Yamé valley deposits, established from the architectural element analysis of
162 [Miall \(1996\)](#) and combined with grain-size analyses ([Table 1](#), [Fig. 2](#)).

Lithofacies assemblages (Miall, 1996)	Description	Other features	M	C99	Grain Size Group	Dessication index *	Current mode of transport	Depositional environment interpretation
Gh, Gt	Horizontal to cross-bedded gravel with cobbles and mud balls		600-2000	4000-20000	A, B	-	Rolling, saltation	Midchannel, lateral gravel bars and bedforms
Sp, Sl	Horizontal to cross-bedded coarse sand with gravels		300-1200	1000-4000	B, C	-	Saltation and rolling	Midchannel, lateral sand bars and bedforms
Sh	Laminated fine sand to coarse sand	Alternating with Fl	70-300	400-2500	C	-	Saltation and suspension	Sand sheet deposited out of main channel during flood events
Sm	Massive sandy-silt to medium sand	Redoximorphic features	50-300	300-700	C	2	Suspension and saltation	Sand flooded out over the alluvial plain
Fl	Laminated silty sand to fine sand	Alternating with Sh	15-200	300-700	D	1,2	Suspension	Fine sediments deposited in floodplain /pond during the low stage
Fsm	Laminated greyish silt to silty sand	Organic remains, redoximorphic features	20-100	100-250	E	1-3	Suspension	Swampy floodplain or/and ponds
Fm	Massive dark organic silt	Rich in organic matter / sometimes desiccation cracks	4-20	80-250	E, F	0,2,3	Uniform suspension during falling	Standing pools of water
-	Massive sandy silt to coarse sand	Sometimes with paedogenic features	100-300	800-1200	D	-	-	Colluvial deposits

*** Level of desiccation of floodplain and pond (Lespez et al., 2011): 0 = lack of desiccation figures and seasonal pattern; 1 = rhythmic sediments testify to a seasonal pattern of sedimentation; 2 = development of oxidation borders; 3 = desiccation cracks; 4 = floodplain paleosoil**

and interpretation

177 Facies assemblages were classified based on their grain-size, texture, structure, colour
178 and biogenic remains and composition of alluvia that are characteristic of the context of
179 sediment deposition (channel, floodplain, pond, etc.) and fluvial style (braided, wandering,
180 meandering, floodout, etc.). Facies are subdivided into four depositional environments
181 distinguished by their modes of deposition (Fig. 2). Four facies are interpreted as channel
182 deposits (Gh, Gt, Sp, Sl), four as floodplain deposits (Sh, Sm, Fl, Fsm) and one facies is
183 characteristic of standing pools of water (Fm). One other facies is interpreted as colluvial
184 deposits. It includes various facies formations with a silty matrix without clear sediment
185 organization. For the channel deposits, the different subfacies permit the qualification of the
186 stream power of the river (high, medium, low energy) (Fig. 2). For the floodplain deposits,
187 another feature has been used to refine interpretation, the desiccation index (DI), developed
188 by Lespez et al. (2011). Based upon the identification of the effects of the intensity and/or
189 length of the dry season on the floodplain and pond deposits this index compares the impact
190 of the dry season on the floodplain landforms during the Holocene. This index has four levels
191 for intensity of desiccation (Table 1; Lespez et al., 2011). It is a good indicator of the
192 characteristics of the dry season and reveals the hydrological level of the valley floor for the
193 different sections and time slices.

194 **3.3. Chronology and sediment storage estimation**

195 The chronology of this study is based on 27 additional radiocarbon dates obtained on
196 charcoal or on sediments (Table 2). The measurements were performed by the AMS ¹⁴C
197 laboratories in Erlangen (Erl), Germany and in Miami, United States (Beta). Radiocarbon
198 dates were calibrated using Oxcal (4.2 version) with the IntCal13 atmospheric calibration
199 curve (Reimer et al., 2013). The chronology used in this paper was identified in accordance
200 with the chronological pattern previously established at Ounjougou (Huysecom et al., 2009;
201 Ozainne et al., 2009).

202

Location	Lab.code	Section	Depth (cm)	Material	Method	Depositional environment	BP +/-	$\Delta^{13}\text{C}$ ‰	Calibrated dates BP (2 σ)
Doucombo	Erl-14729	CP34	283	Wood	AMS	Channel	6066 +/- 46	-24,42	7155-6786
Doucombo	Erl-14728	CP 33	292	Charcoal	AMS	Channel	4468 +/- 38	-25,68	5291-4972
Doucombo*	Erl-15477	C1	537 -539	Sediment	AMS	Pond	2695 +/- 56	-18,3	2925-2738
Doucombo*	Erl-15479	C3	668	Charcoal	AMS	Channel	1645 +/- 43	-26,8	1690-1413
Doucombo	Erl-14726	CP 24	206	Charcoal	AMS	Colluvial	416 +/- 35	-23,84	526-326
Doucombo	Erl-15478	C3	335	Charcoal	AMS	Floodplain	216 +/- 42	-25,3	425--4
Doucombo	Erl-14727	CP 23	288	Charcoal	AMS	Colluvial	138 +/- 34	-23,86	281-6
Doucombo	Erl-14723	CP 2	165	Charcoal	AMS	Floodplain	52 +/- 39	-25,91	261-24
Allaye	Erl-14717	CP 16	180	Charcoal	AMS	Colluvial	4377 +/- 36	-26,64	5041-4858
Fiko*	Erl-13738	CP4	226	Charcoal	AMS	Colluvial	2442 +/- 53	-27,4	2709-2353
Fiko*	Erl-13402	CP1	170	Charcoal	AMS	Colluvial	2085 +/- 44	-23,3	2292-1933
Fiko	Erl-13740	CP13	240	Charcoal	AMS	Colluvial	893 +/- 40	-25	916-732
Fiko	Erl-13739	CP13	220	Charcoal	AMS	Colluvial	845 +/- 40	-24,2	904-681
Kéma	Erl-14720	CP 18	290	Charcoal	AMS	Floodplain	479 +/- 37	-25,42	619-479
Fiko	Erl-13401	CP2	111	Charcoal	AMS	Colluvial	339 +/- 39	-22,9	488-308
Kéma	Erl-14718	CP 18	161	Charcoal	AMS	Floodplain	203 +/- 34	-24,61	307--4
Kéma	Erl-14719	CP 18	194	Charcoal	AMS	Floodplain	127 +/- 38	-27,21	278-8
Baïma*	Beta-298317	C1	750-752	Sediment	AMS	Swampy floodplain	2460+/-30	-16,4	2716-2357
Baïma*	Beta-298316	C1	570-572	Sediment	AMS	Floodplain	1930+/-30	-17,5	1947-1820
Baïma*	Erl-15486	C1	420-422	Sediment	AMS	Wetland	1630 +/- 66	-16,4	1695-1385
Baïma	Erl-15487	C3	238-240	Sediment	AMS	Wetland	923 +/-43	-14,3	926-681
Baïma	Erl-13741	C1	256	Charcoal	AMS	Wetland	281 +/- 42	-24,6	473- -1
Samoloye	Beta-298318	C2	265-267	Sediment	AMS	Wetland	1100 +/-30	-14,7	1063-937
Sampara	Erl-15488	C3	354-356	Sediment	AMS	Channel	4055 +/-47	-20,1	4808-4421
Sampara	Erl-13745	C2	371 - 375	Sediment	AMS	Wetland	3316 +/- 41	-21,9	3676-3449
Sampara*	Erl-13744	C2	264 - 266	Sediment	AMS	Wetland	2473 +/- 40	-16,7	2715-2364
Sampara*	Erl-15489	C4	440	Charcoal	AMS	Channel	1664 +/-43	-27	1695-1418

* *Published in Garnier et al., 2015*

203

Table 2: Radiocarbon dates obtained on deposits of the Yamé valley

204

205 Setting aside Ounjougou, seven complete cross-sections surveys have also been carried out
206 in the Yamé valley: two in the middle valley, four in the lower valley and one in the inland
207 delta domain (Fig.1). The stratigraphic study of deposits, established from the investigations
208 carried out in the field and laboratory and from available dating, allows for the
209 characterization of the thickness of the sedimentary fill for each period and reaches studied.
210 Because the fluvial architecture is relatively stable and coherent within each different scale,
211 we decided to quantify the volume of sediment stored for the whole valley. For each reach,
212 the fluvial architecture observed was extrapolated from boreholes and outcrops data. Despite
213 its exploratory nature, this analysis provides an idea of the valley floor filling rhythms over the
214 last millennia. The calculating method is based on five steps. The first two steps were
215 conducted in the field. For each studied reach (1) the identification of the geomorphological
216 units and (2) the establishment of the chronostratigraphy was undertaken. The next step
217 consists of extrapolating the thickness of the sediment storage for all 500m sections and
218 calculating the volume for different time slices. However, some adjustments were made
219 based on local observations. For example, periods of incision do not concern the entire
220 surface of the floodplain but only of the channel. Thus, the thickness of the removed
221 sediment was multiplied by the surface of the channel to estimate the alluvial storage in the
222 valley floor. Similarly, for section 2, sediment storage was only calculated for the
223 Ounjougou's reach because storage is effective only there due to favorable local
224 geomorphological conditions (Rasse et al., 2006; Lespez et al., 2008, 2011). However, in
225 order to compare the volumes and improve interpretation, the data were normalized. The
226 volume of stored sediment is indicated per year and per km.

227 **4. Results and interpretation**

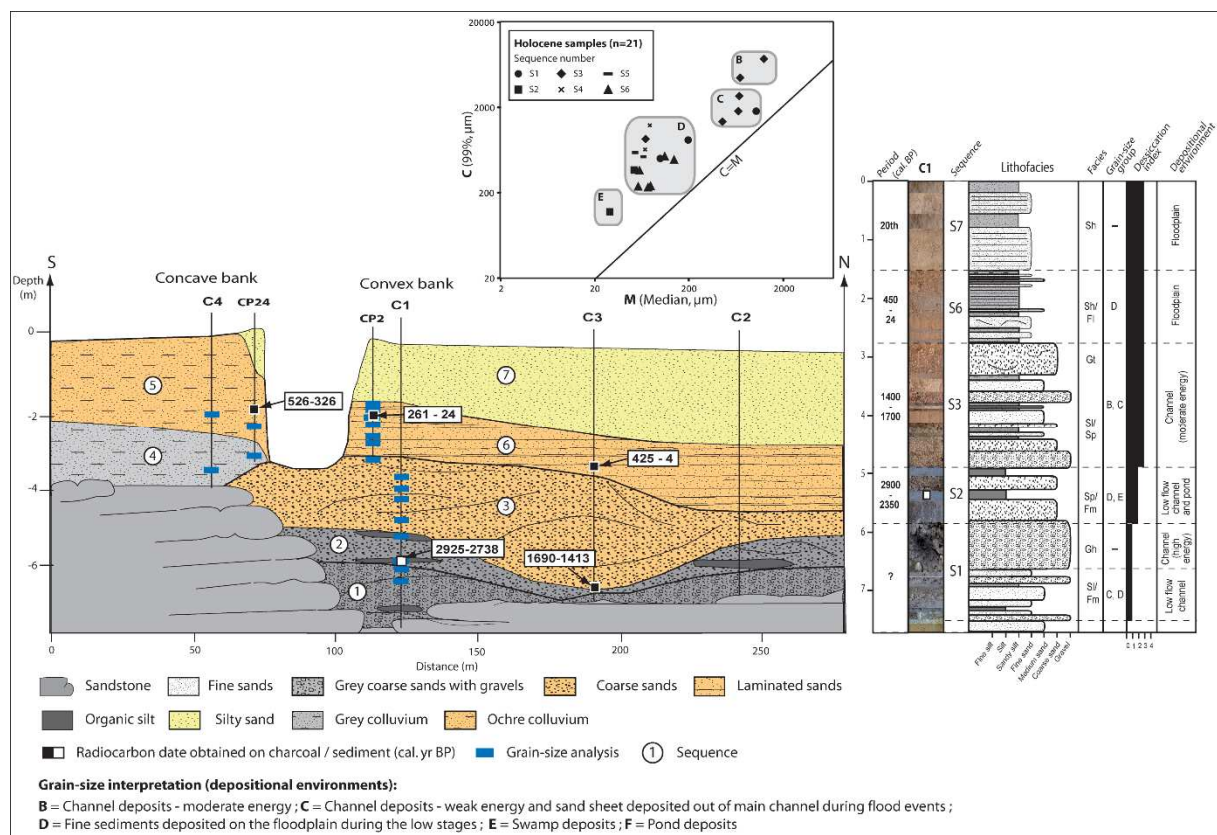
228 **4.1. Chronostratigraphy of the deposits by reach**

229 **4.1.1. The midcatchment**

230 The midcatchment, located between Bandiagara and Goundaka, corresponds to a
 231 meandering irregular planform-controlled discontinuous floodplain River Style (Fig. 1). The
 232 investigations were primarily conducted by cores in meandering lobes and by outcrop profiles
 233 in ravines and along the Yamé River. The sedimentary filling, about 3–4m deep above
 234 sandstone, corresponds to a stacking of alluvial sequences fed by colluvial deposits.

235 4.1.1.1. Doucombo cross-section

236 The cross section of Doucombo corresponds to a meander characterized by a wide
 237 floodplain and alluvial sedimentation on the convex side (Figs. 1 and 3). Four boreholes and
 238 several outcrop profiles permitted the identification of five sedimentary sequences. On the
 239 convex bank, a detrital sequence, 1.5m thick, has been identified at the bottom.



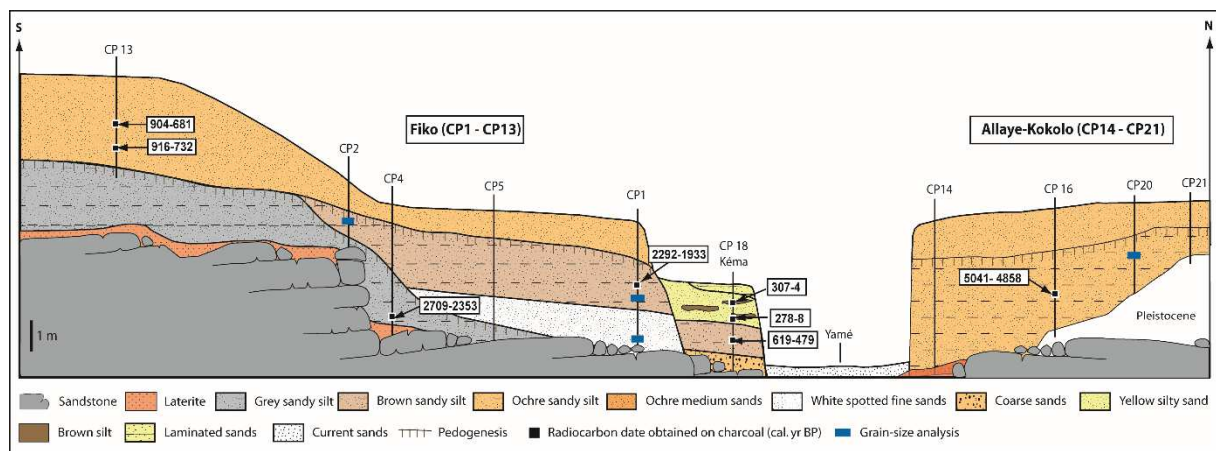
240
 241 **Fig. 3: The cross-section of Doucombo**

242
 243 The lower sequence (S1), 90 cm thick and not dated, can be characterized by fine sand
 244 beds (S1) with some blue compact laminated organic silts, indicating waterlogged and

245 reducing conditions (Fm). It is overlain by blue-grey coarse sands to gravels (Gh). In
246 contrast, the second sequence (S2), 60 cm thick and dated to 2925-2738 cal. BP, contains
247 finest sandy deposits with a planar structure (Sp), intercalated with compact organic silts
248 (Fm). These deposits reflect the channel's sediments transported during high flood flows for
249 the coarser layers (Gh) or during more moderate flooding for the finest deposits (Sl/Sp).
250 However, the color of the deposits and the presence of several dark organic silty layers
251 without desiccation cracks (Fm) indicates a high water table all year round with many
252 standing pools in the valley bottom. The contact with the next sedimentary sequence (S3) is
253 clearly erosional. This incision, 1.5m deep in cross section into older deposits, corresponds
254 to a period between 2925-2738 and 1690-1413 cal BP, a date obtained from the bottom of
255 the top sequence. This second detrital sequence, 3m thick, corresponds to ochre coarse
256 sand and gravels with planar or cross-bedding structure (Sl/Sp/Gt). The red - rust color of the
257 deposits indicates an iron oxidation state reflecting contact of the sediments with air. Thus,
258 compared to the previous period, there was a drop in the water table level. Sediments
259 correspond to coarse sand containing some gravel beds that reflect the development of
260 medium and lateral bars and a moderate flood energy. On the concave bank, a colluvial
261 sedimentation 3m thick has been updated (S4 and S5). The oldest sequence is constituted
262 by grey silty sands containing pulverulent iron concretions, while the following one, dated to
263 526-326 cal BP, is characteristic of an alternation of ochre-brown silty sand layers with
264 numerous iron concretions. On the convex bank, the sedimentation is characterized by a
265 much more recent laminated sequence (S6), showing the alternation of silty sand to fine
266 sands (Sh/FI). Two dates are available for this sequence, 425-4 cal BP and 261-24 cal. BP.
267 These deposits, 1m thick, are interpreted as sand sheet deposits spread outside of the main
268 channel on the floodplain during moderate-energy flood flows. At the top of both banks, a
269 sequence (S7) 1 to 2m thick, corresponds to the current hydro-sedimentary pattern revealed
270 by laminated silty sands (overbank deposits).

271 **4.1.1.2. Fiko cross section**

272 In this part of the valley, three topographic levels have been identified: the upper glaciais,
 273 the low glaciais and a low terrace (Fig. 4). Nineteen outcrop profiles were carried out along the
 274 Yamé River and in the ravines. For the glaciais, the earliest available date, 5041-4858 cal. BP,
 275 comes from the ravine of Allaye-Kokolo, located on the right bank of the Yamé. The
 276 sedimentary sequence, 1 to 4m thick, is characteristic of ochre silty sands containing gravels.
 277 The nature and sedimentary structure indicates a leached ferruginous paleosol developed on
 278 the erosional levels of Pleistocene glaciais.



279

280 **Fig. 4: Composite cross-section of Fiko**

281

282 From the edges of the Holocene floodplain, eleven outcrop profiles were identified in the
 283 Ravine of Fiko, located a few kilometers downstream on the left bank of the Yamé. The
 284 oldest sequence recorded at the bottom corresponds to grey sandy silt, 1 to 2m thick,
 285 including many charcoal particles. The date of this sequence, rich in pottery sherds, has
 286 been established by radiocarbon dating to 2709-2356 cal. BP. The sedimentary
 287 characteristics and the grey-blue color of these deposits suggest a pseudo-gley paleosoil
 288 dominated by an excess of water. This sequence is covered by white fine sands with
 289 numerous ochre marks. These sediments can be interpreted as overbank deposits fed by
 290 colluvial sediments which were thereafter subject to pedogenic processes. The
 291 characteristics of the basal mass of these deposits is probably the result of an oblique

292 leaching. This paleosoil is then topped by a relatively homogeneous sequence characterized
293 by medium to coarse sands, dated to 2292-1933 cal. BP.

294 At the top of the glacis, there is a sequence of fine red sands reaching a thickness of 2m
295 dated by two charcoal samples to 916-732 cal. BP and 904-681 cal. BP. Similar deposits
296 have been observed on the right bank at Allaye-Kokolo.

297 The low terrace, located at Fiko on the right bank and on the left bank at Kéma upstream, is
298 much more younger. At the bottom, it corresponds to ochre coarse sand. Above, there are
299 colluvial sediments dating to 619-479 cal BP. They are overlain by floodplain deposits
300 characterized by fine to medium sand containing lenses of brown silt. Two dates place its
301 establishment around the last three centuries (Tab. 1; 307-4 cal. BP and 278-8 cal. BP).

302 ***4.1.2. The lowland plain***

303 From Goundaka, the fluvial morphology of the landscape changes. The sandstone plateau is
304 replaced by glacis, which now occupy the whole landscape. We observed the development
305 of an unconfined valley whose width increased greatly. Moreover, the very low slope (0.4 ‰)
306 of this zone promotes sediment storage. Two river styles can be differentiated in this section
307 of the valley (Fig. 1).

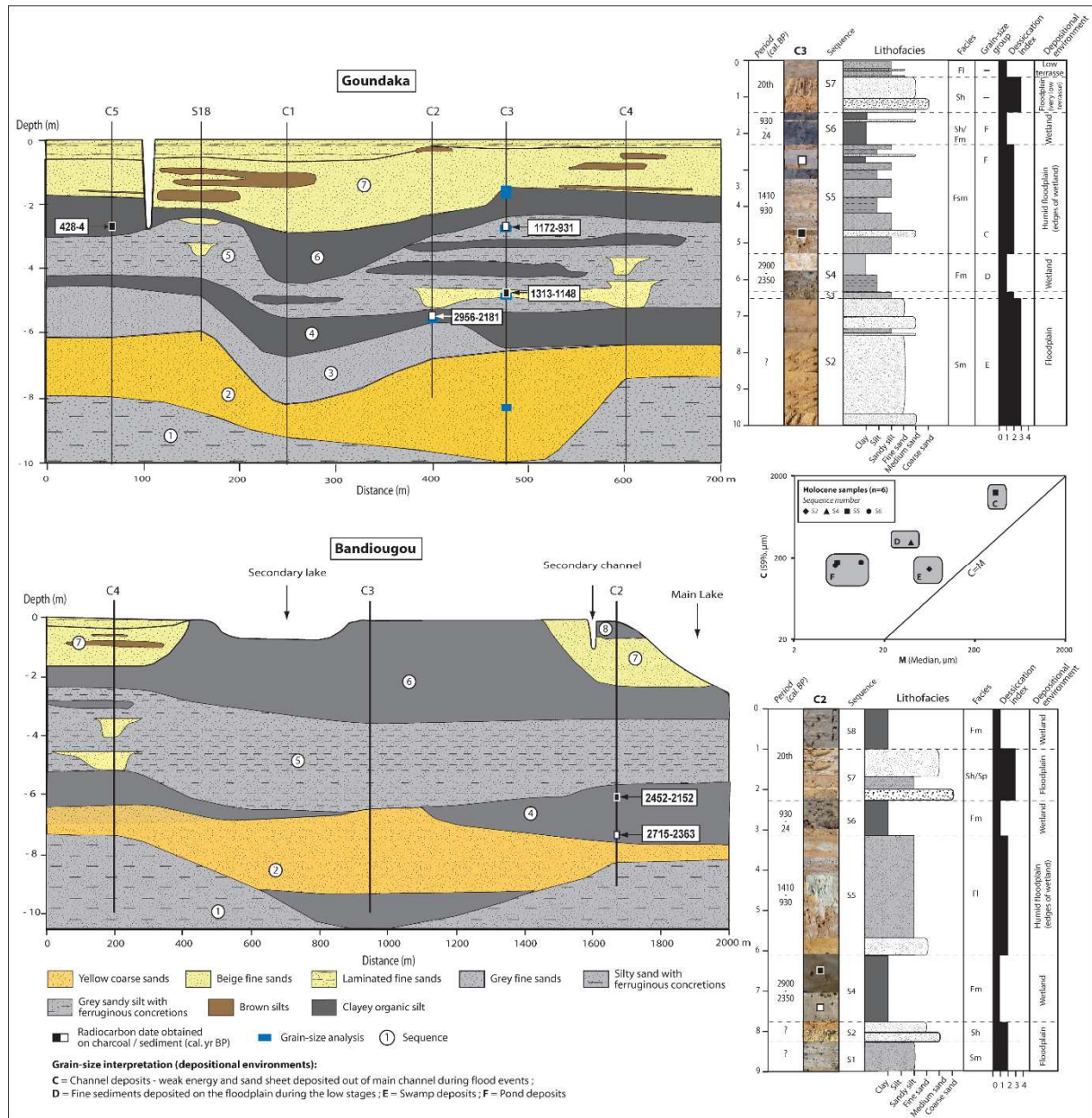
308 **4.1.2.1. Goundaka-Bandiougou cross section**

309 Located upstream of the lower valley, the Goundaka-Bandiougou section is characterized by
310 specific hydro-sedimentary dynamics. Situated on the left bank of the Yamé, the
311 Bandiougou's wetland is approximately 1 km² during the wet season. The lake is fed by two
312 major tributaries coming from the north of the watershed (Fig.1). However, during large
313 floods, the Yamé River can flow into the lake and become a tributary of the Bandiougou's
314 Lake. The Goundaka's reach is located at the interface between the Yamé River and the
315 lake.

316 At Goundaka, eight boreholes and two auger holes were undertaken. The chronostratigraphy
317 study indicates seven different sequences (Fig. 5). The oldest one, 2m thick, corresponds to

318 grey sandy silt with ferruginous concretions (Sm). These sediments are not dated but are
 319 older than 2956-2181 cal. BP, the first date provided by the upper sequence. They are
 320 overlain by heterometric yellow-brown sands. This sequence can be interpreted as
 321 sediments carried by flows that lose their velocity and competence as they spread over a flat
 322 floodplain and deposit their sediment load (Sm).

323



324

325

Fig. 5: Cross sections of Bandiougou and Goundaka

326

327 Sedimentary records of the following sequence are thinner in depth (m) and organic. In the
328 lower part, there is a layer of grey sands (Sm) covered with organic silt (Fm). These were
329 deposited by decantation in wetland environment such as lake or ponds.

330 The above sedimentation corresponds to silty sandy deposits including finer layers. It is
331 dated to the top of 1172-931 cal. BP. This evidence suggests a swampy, depositional
332 environment of wetland margins that are subject to low flood flows (Sf). However, these
333 deposits are also impregnated by ochre-rust marks indicating an oxidizing environment.
334 There is, in some places (C3, C4 and S18), a sandy layer indicating a return to fluvial
335 dynamics dating to 1313-1148 cal. BP at C3.

336 The following sequence reveals organic silt deposited by decantation (Fm). This corresponds
337 to the development of swampy - lacustrine conditions for all of the Goundaka reach. These
338 deposits are dated at C5 to 428-4 cal. BP. They are also intercalated with sandy deposits
339 (Sp) suggesting the presence of a wandering channel throw into the lake.

340 Finally, the top of the sedimentary filling is composed of an alternation of laminated sands
341 (FI), that come from the overflow of the Yamé and its tributaries during contemporary flood
342 episodes.

343 At Bandiougou, the same alluvial pattern as at Goundaka is observed (Fig. 5). At the bottom,
344 we observed grey sandy silt sediments (Facies FI), reflecting a wide floodplain inundated by
345 low flows. At the core C3, a fine silty clay sequence (Fm) indicates the development of a
346 wetland. It is overlaid for all cores by yellow-red sands suggesting a suspended load
347 deposition. Thus, we can assume they have been deposited by overflows within this vast
348 floodplain (floodout). Two dates are available (2715-2363 cal. BP and 2452-2152 cal. BP)
349 which are similar to Goundaka for the same sequence. This indicates the presence of a large
350 wetland during the first millennia BCE.

351 The next sequence, 3m thick, consists of grey fine sand and has also been observed at
352 Goundaka. This sedimentary facies is associated with the sequence 5 (Fig. 5). The structure
353 correspond to massive sands (Sm) that have been transported by overflow and deposited in
354 the floodplain by the reduction of the flow velocity. However, in the west, near the present-

355 day Yamé, sedimentation appears different. This sequence of grey silty sand is intercalated
356 with detrital laminae (Sp), characteristic of channel deposits during episodes of flooding and
357 organic clay lenses (Fm) that suggests the presence of wetlands in the floodplain. They can
358 also result in sedimentation in pools or from an extension of Lake Bandiougou for certain
359 periods of time.

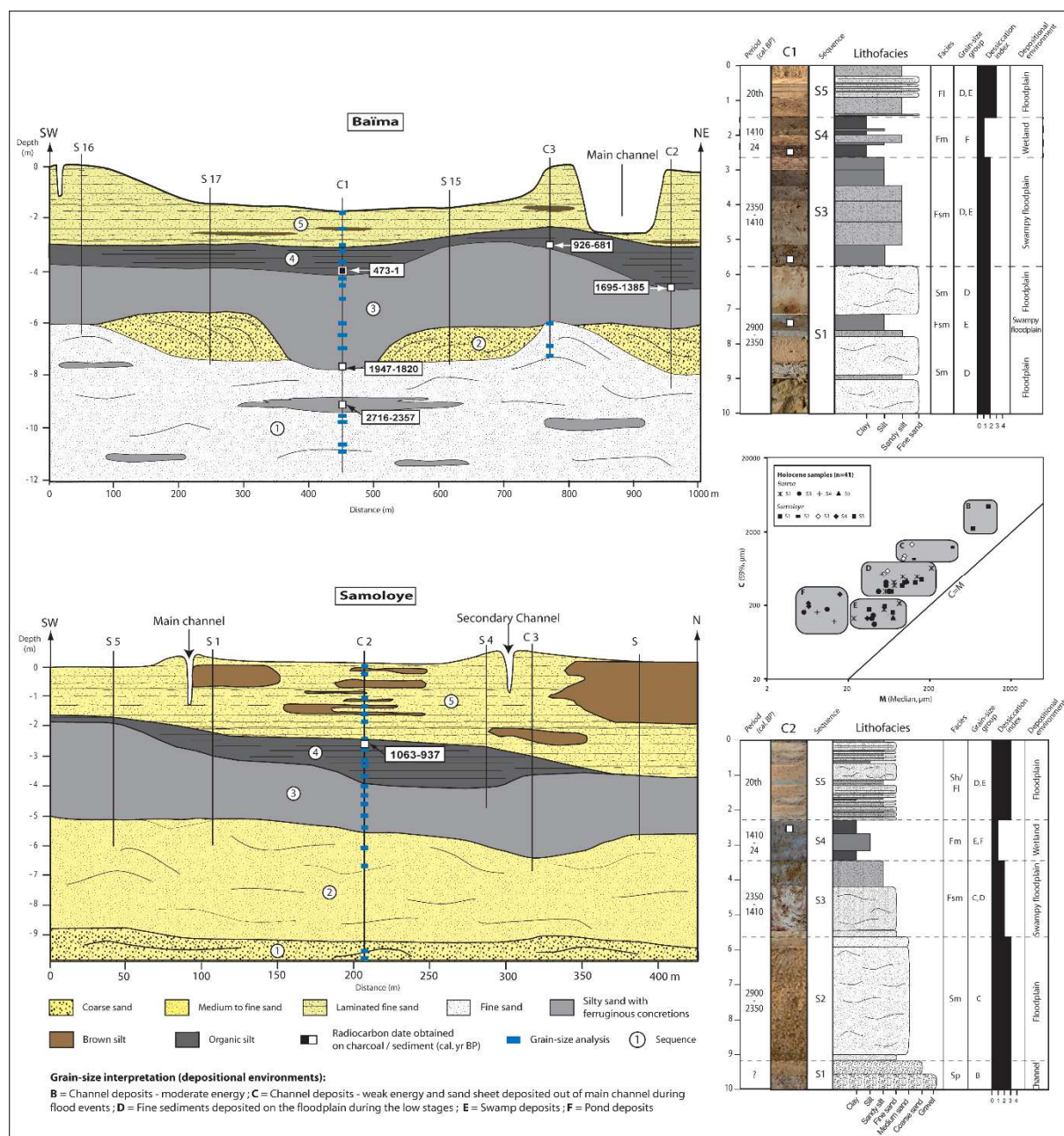
360 They are then topped by an organic clay sequence usually thick depending on the location of
361 the coring (1-3m). According to the dates available at Goundaka, we assume that this
362 sequence corresponds to the last millennium. The fine organic sedimentation without
363 desiccation cracks (Fm) indicates the development of a permanent wetland from this time
364 onwards. To the west, the last meter observed corresponds to the establishment of the
365 current system with sandy sediments that originated from the overflow of the Yamé during
366 the last few centuries. However, to the east, near the present lake, alluvial sediments with
367 coarse beige sands (Sl / Sh) have been identified. These probably came from the channel of
368 the tributary, now located just a few meters from the C2 core. At the top, contemporaneous
369 lacustrine deposits are observed (Fm).

370 Thus, for at least the last two millennia the Goundaka's reach was characterized by
371 sedimentation that fluctuated between alluvial or swampy-lacustrine sequences.

372 **4.1.2.2. Baïma cross section**

373 The Baïma cross-section is located at the beginning of the lower valley, just after the
374 confluence with the last tributary of the Yamé River. Hand auger (S16, S17 and S15) and
375 boreholes (C1, C2, and C3) enabled the identification of five sedimentary sequences (Fig. 6).
376 The sedimentation of the bottom sequence was composed of 5m thick massive fine silty-
377 sand (Sm) with some silty sand patches with ferruginous concretions (Fsm). These are
378 interpreted as swamp deposits in an alluvial plain overlaid by sand sheet flooded out during
379 low energy flood flows. It can be related to a suspended load transported by a energetic fluvial
380 system. This sequence dated to 2716-2357 cal BP and is characterized by a strong 2m thick
381 erosion occurring between 2716-2357 and 1947-1820 cal BP. However, this period is

382 recorded in the sedimentation filling by coarse sand (Sp) transported in a channel by medium
 383 energy flood flows. It is overlaid by 2m thick sandy silt sediments (Fsm) interpreted as
 384 swampy floodplain deposits and dated from 1947-1820 to 1695-1385 cal BP. Thus, a system
 385 of lower energy characterized by the development of wetlands with 1m thick fine and organic
 386 sedimentation (Fm) was recorded and dated between 1695-1385 and 473-1 cal BP. The last
 387 sequence, 2m thick, corresponds to the alternation of fine sands and sandy silt (FI) which are
 388 the current overbank deposits.



389

Fig. 6: Cross sections of Baïma and Samaloye

390

391

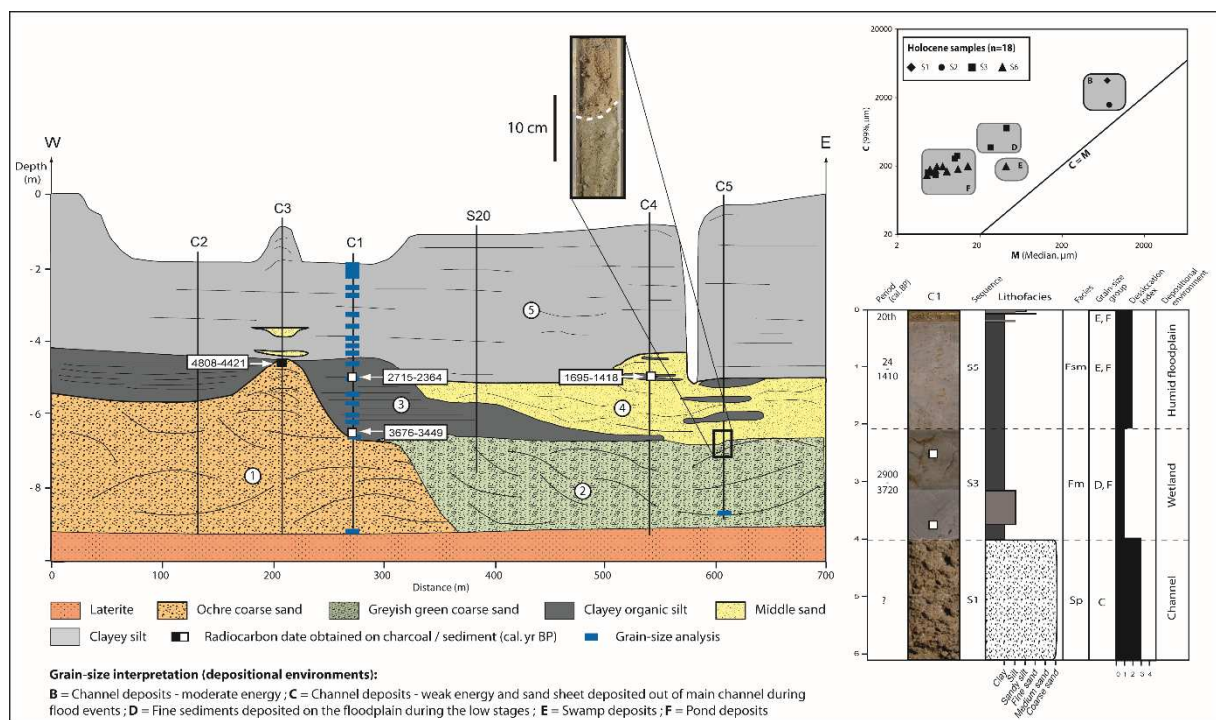
392 4.1.2.3. Samoloye cross section

393 The Samoloye's reach is located 15 km downstream of Baïma. The architecture of the
394 alluvial filling was established by four hand auger (S1, S3, S4 and S5) and two boreholes (C2
395 and C3) (Fig. 6). Four sequences have been identified. Setting apart the two bottom
396 sequences, the infill is similar to those observed for the section at Baïma. At the bottom,
397 sediments correspond to coarse sand (Sp) interpreted as channel bars transported by high
398 energy flood flows. It is overlaid by a 4m thick medium sand sequence with massive structure
399 (Sm) which indicates a deposition by suspension during low energy velocity. Before 1063-
400 937 cal BP, a 2m thick sandy silt (Fm) sequence was covered by a 1m thick dark organic silt
401 (Fm) which has been interpreted as swamp deposits and dated to 1063-937 cal BP. Finally,
402 from the top we observe a filling of the valley bottom with sand sheet and ponds deposits
403 (Sh/FI) corresponding to the current pattern.

404 4.1.3. The Niger Inland Delta domain

405 Downstream of the valley of the Yamé River, a few kilometers away from the confluence with
406 the Niger River, the reach of Sampara has been the subject of five boreholes (C1, C2, C3,
407 C4, C5) and one outcrop profile (CP19) (Fig. 7). These investigations permit the identification
408 of five sedimentary sequences. At the bottom, lateritic deposits are overlain by two detrital
409 sequences. The oldest one is mainly developed on the west side of the cross-section and is
410 characterized by a 4m thick ochre coarse sand (Sp) transported in a meandering channel
411 during high energy flood flows. The upper surface of this sequence is dated to 4808-4421 cal
412 BP. The following one is slightly incised within on the east side of the cross section. The 2m
413 thick blue-green coarse sand to gravels (Gh) including some layers of organic clayey
414 deposits (Fm) is interpreted as deposits characteristics of wandering channels including
415 many standing pools in the valley bottom. It is covered by 1.5m thick silty clayey sediments

416 (Fm) interpreted as standing pool. This sequence, rich in organic matter, was dated on the
 417 base to 3676-3449 cal BP and at the top to 2715-2364 cal BP. The contact with the following
 418 sequence is erosional on the east of the cross-section. The incision is dated between 2715-
 419 2364 cal BP and 1695-1418 cal BP. This 1.5m thick, sequence developed east of the cross
 420 section, corresponds to medium yellow sands planar structure (Sp), and intercalated with
 421 organic silt lenses (Fm). Interpreted as a return towards a fluvial system with an average
 422 energy, this meandering system is dated to 1695-1418 cal. BP. Finally, the last sequence,
 423 4m thick, presents overbank silt deposits (Fsm) corresponding to the current hydro-
 424 sedimentary pattern, a swampy environment that dries up seasonally as shown by the
 425 oxidation marks. Thus, these sediments, deposited since the middle of the second
 426 millennium CE, come from the overflow by slow currents during the flood of the Yamé and
 427 Niger and have remained suspended in water for several months.

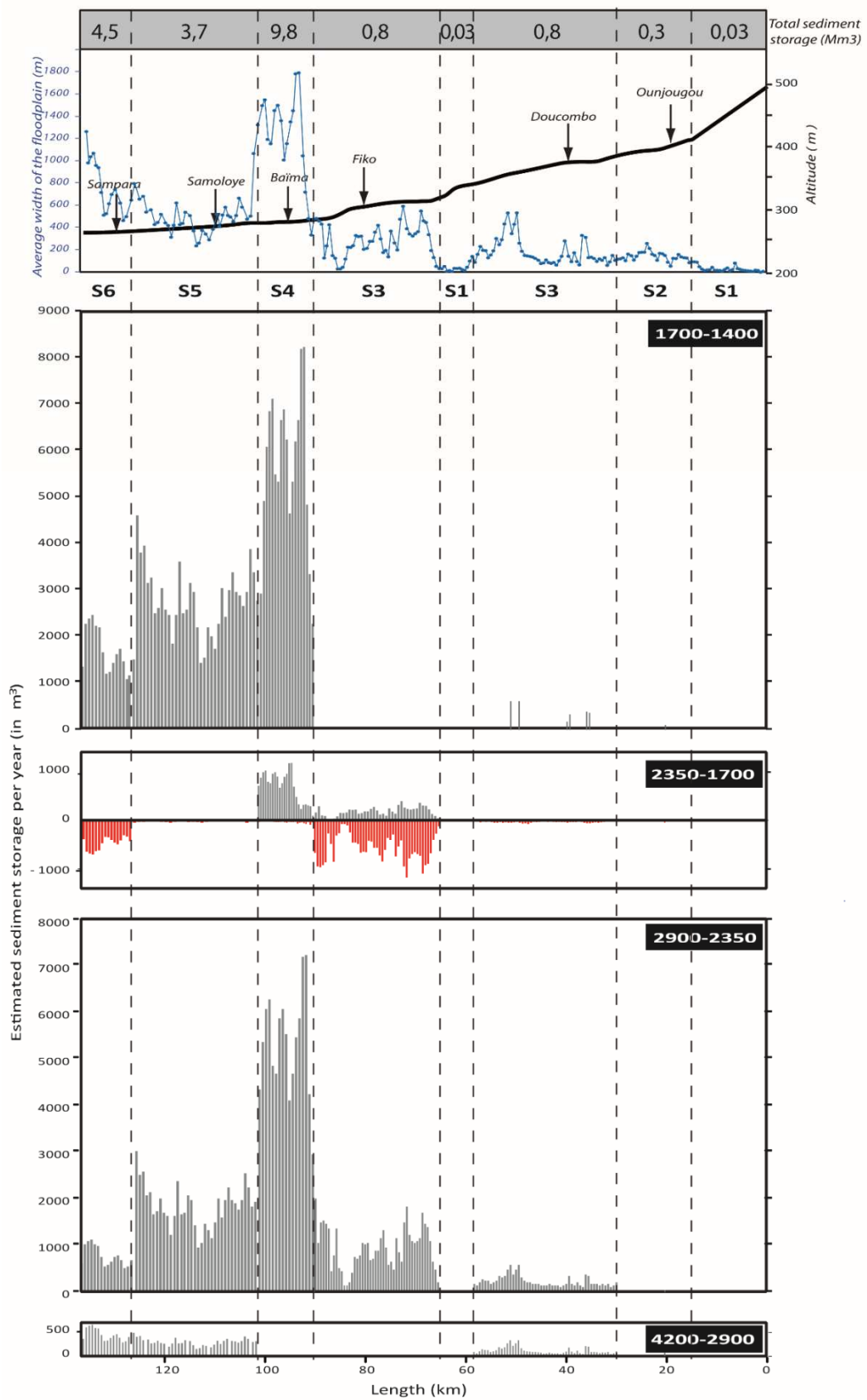


428 **Fig. 7: Cross-section of Sampara**

429
 430
 431 **4.2. From upstream to downstream: fluvial dynamics and sediment**

432 From the Late Holocene onwards (4200 cal. BP to today) sedimentary archives have been
433 preserved for the whole Yamé valley and have allowed the reconstruction of the longitudinal
434 fluvial dynamics. The total Holocene sediment stored in the Yamé valley is estimated at 292
435 million m³ (Fig. 8.a). Most of the sedimentary filling has been recorded in the lower valley
436 (sections 4 and 5) with an estimation of about 200 million m³.

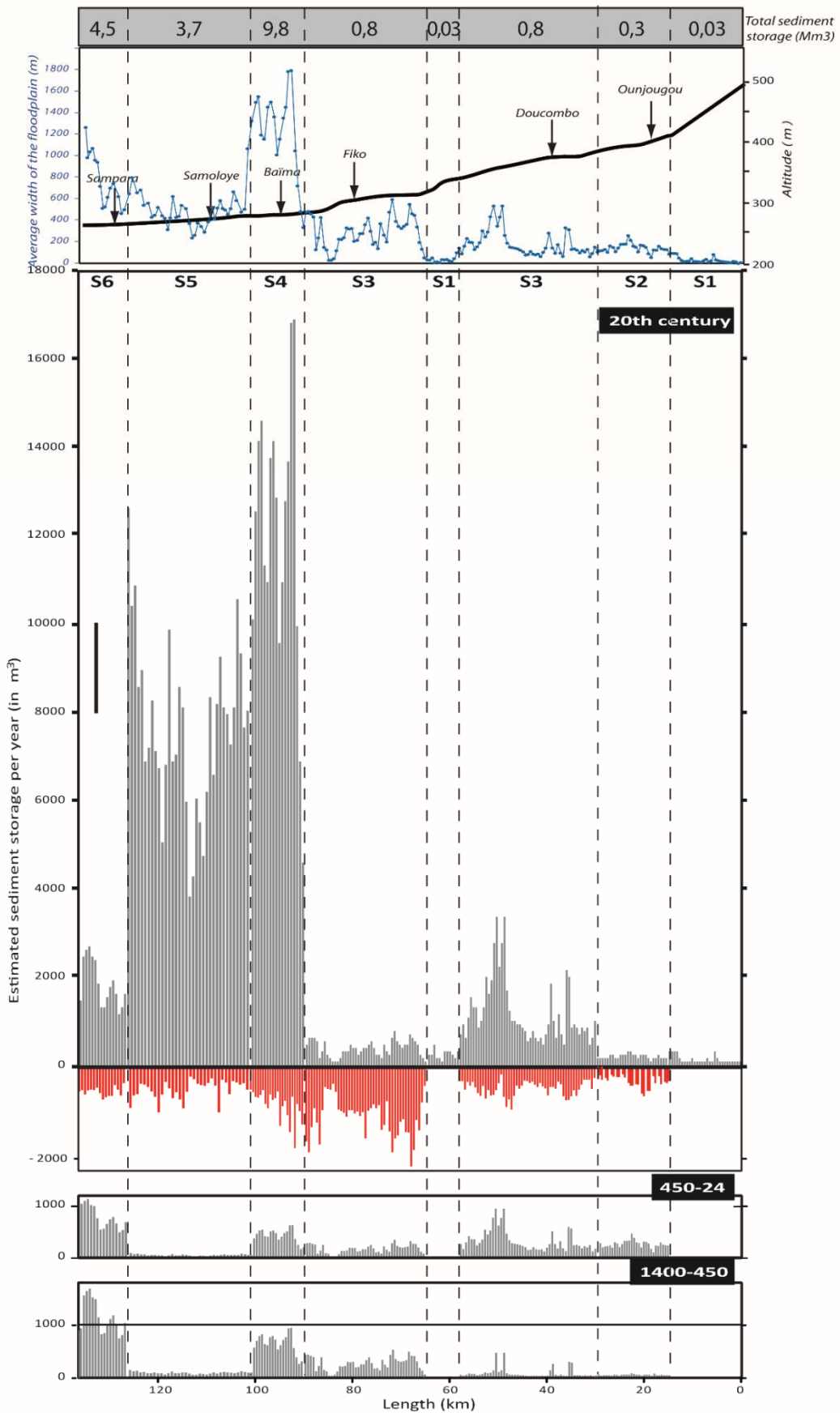
437 According to the same time slices dating from the beginning of the Late Holocene
438 onwards, figure 8 shows the sedimentary storage of each section estimated per year and per
439 500m section. Figure 9 depicts the changing nature of river style and process zones (alluvial
440 sediment accumulation, transfer and source zones) within the Yamé fluvial system.



441

442 **Fig. 8.a: Yamé valley estimated sediment storage (in m³/year) for each 500m**

443 **section long (input in grey bars and output in red bars). Time scale in cal. BP.**



444

445

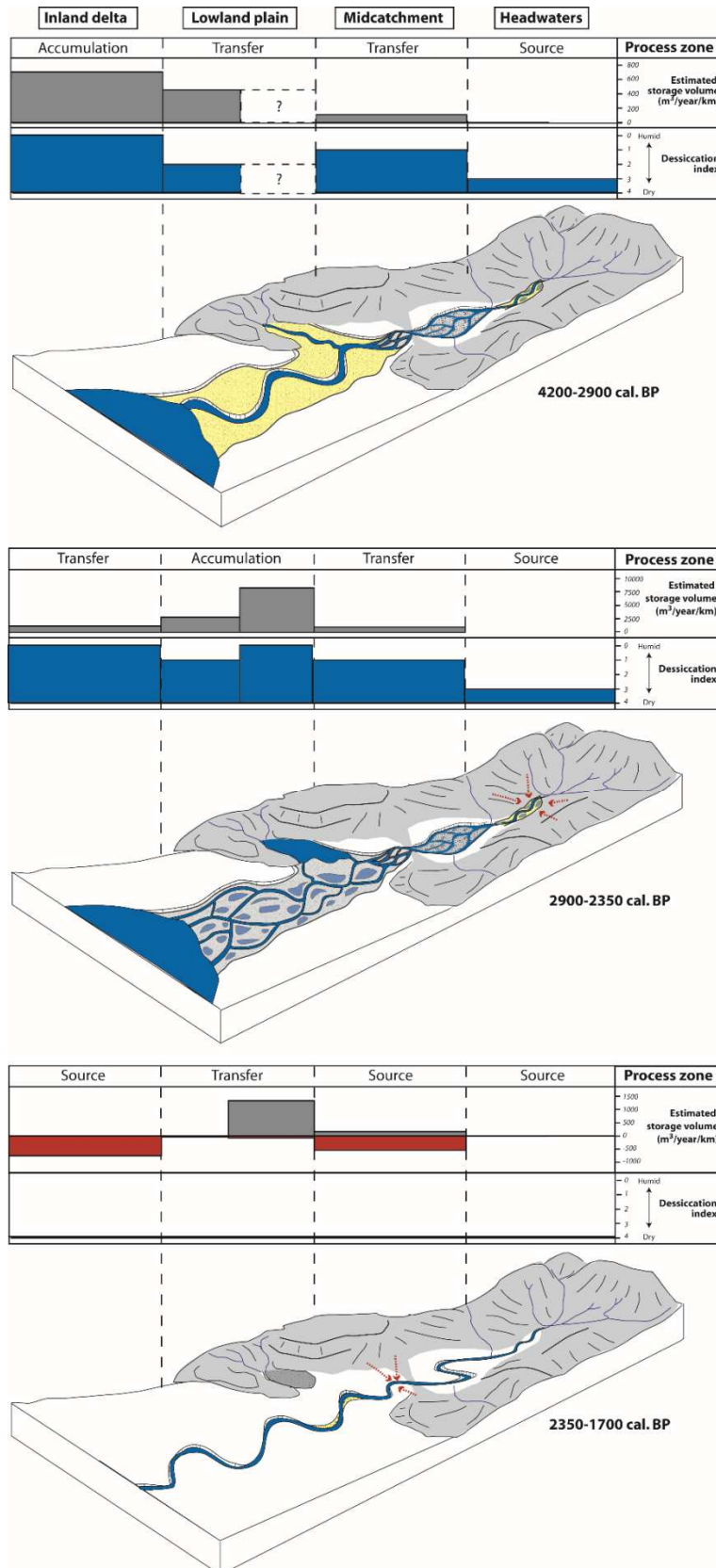
446

Fig. 8.b: Yamé valley estimated sediment storage (in m³/year) for each 500m section long (input in grey bars and output in red bars). Time scale in cal. BP.

447 At the beginning of the Late Holocene (**4200-2900 cal. BP**), the sediment cascade indicates
448 an idealized river system pattern with an increase of sediment storage in the downstream
449 direction. The estimated volume of stored sediment is approximately 24 000 m³/year for the
450 whole valley and progressed from 4 m³/year/km at Ounjougou to 700 m³/year/km by average
451 for section 6 (Fig. 9.a). The middle and lower valley acted as sediment transfer zones as
452 illustrated by their river style, which was characterized by a wandering river in the middle
453 valley and meandering style in the lower valley.

454 During the next period (**2900-2350 cal. BP**) an important change occurred in the pattern of
455 the Yamé valley as shown by the volume of stored sediment which sharply increased,
456 reaching a total of 221 000 m³/year. First, colluvial deposits have been observed revealing
457 the onset of a new process of sediment production. Thus, the sandstone plateau remained
458 as a source and transfer zone while the lower valley was transformed into an accumulation
459 zone. For section 4, sedimentation of fine sands was very important representing an average
460 of 8234 m³/year/km. Then, sedimentation in the valley bottom decreases progressively
461 downstream to an average of 2757 m³/year/km for section 5 and finally almost 1148
462 m³/year/km for section 6.

463 The following period (**2350-1700 cal. BP**) is a key phase in the evolution of the Yamé River
464 system. It corresponds to a deep incision of the channel in the earlier deposits for the entire
465 valley. The total volume of sediment pulsed is about 38 000 m³/year more than the sediment
466 volume stored (24 100 m³/year). This incision is particularly important in the middle valley for
467 section 3, with the export of more than 29 000 m³/year (540 m³/year/km) (Fig. 9.a). It is
468 relatively weak in the lower valley where the export is an average volume of 71 m³/year/km
469 and 40 m³/year/km for sections 4 and 5, respectively. Finally, incision is more intense
470 downstream with a discharge of 745 m³/year/km of sediments. Thus, except for section 4, all
471 sections acted as sediment source areas. However, lateral supplies, attested by the
472 observation of colluvial deposits allowing sediment storage in the middle valley at 9102
473 m³/year (170 m³/year/km). In section 4, sediment storage is about 15 000 m³/year (1 300
474 m³/year/km).



475

476

477

478

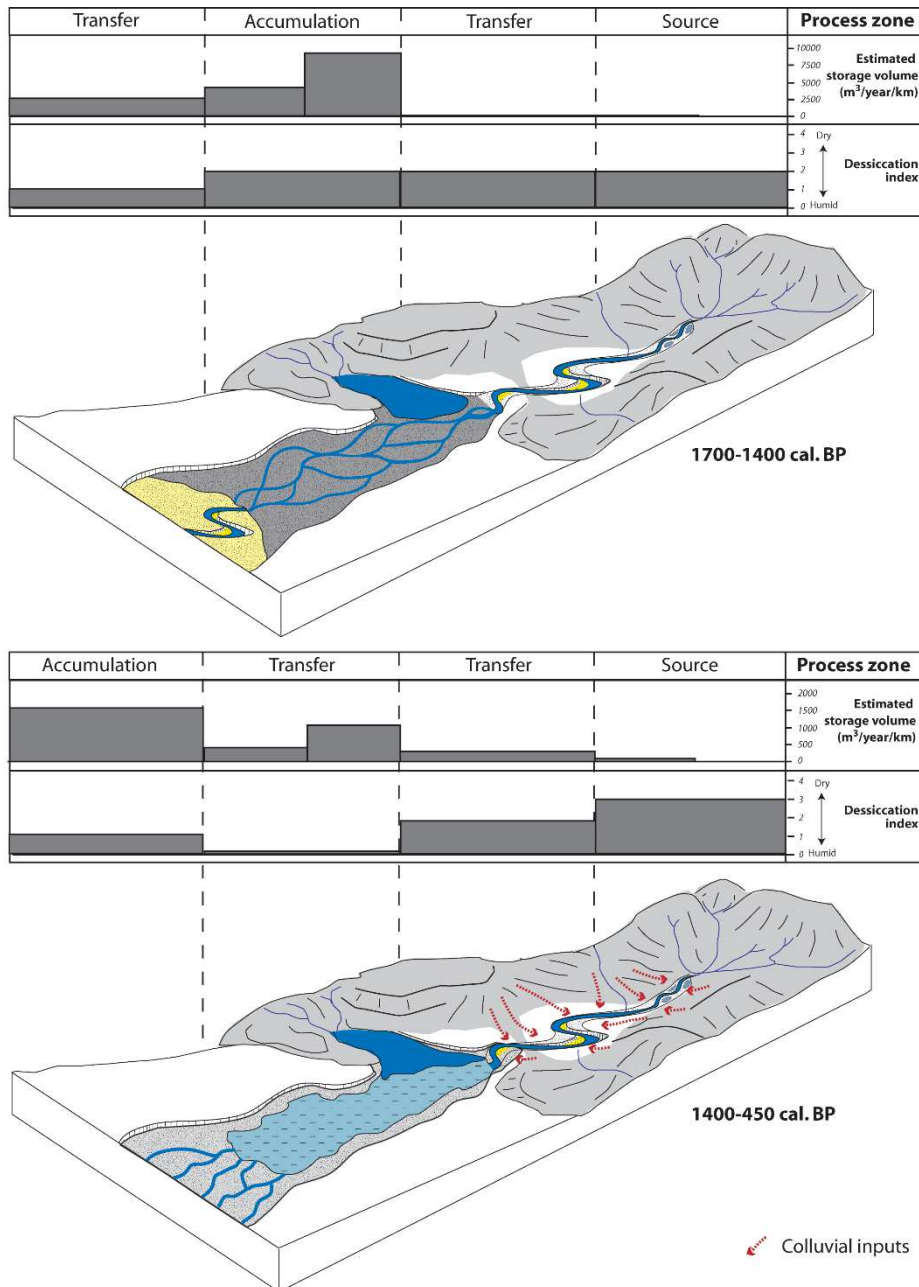
Fig. 9.a: Fluvial dynamics reconstruction along the Yamé valley during 4200-1700 cal. BP. Sediment storage is indicated for each section by an average of m^3 per year and km.

479 The **1700-1400 cal. BP** period indicates a return to an alluvial aggradation into the
480 catchment with the volume of stored sediment slightly higher than during the 2900-2350 cal.
481 BP period with a total of 234 500 m³/year. In the headwaters, the function of the valley
482 remained as a sediment source while the middle valley and the inland delta section were
483 transformed into sediment transfer zones. In response to this sediment influx, the lower
484 valley became again an accumulation zone. The average volume stored in sections 4 and 5
485 was 9357 m³/year/km and 4234 m³/year/km, respectively.

486 The sediment records of the **1400-450 cal. BP** period show an idealized river system pattern
487 with a downstream sediment conveyance throughout the valley. On the sandstone plateau
488 (upper and middle valley), the fluvial style is a meandering river system fed by colluvial
489 deposits indicating a lateral sediment supply. The lower valley was transformed into a
490 sediment transfer zone while the inland delta domain shifted to sediment sinks. Hence, the
491 sediment supply was less important than the previous period as demonstrated by the total
492 volume of stored sediment reaching about 54 800 m³/year.

493 Over the past five centuries (**450-24 cal. BP**), the fluvial system was quite similar to the
494 previous period except for the upstream zone which switched from a source zone to a
495 sediment accumulation zone. Swamp deposits associated with an increase in sediment
496 storage rate indicate that these local swamps acted as sediment sinks. However, the middle
497 valley, illustrated by a meandering channel river style remained a transfer zone. The high
498 record of sediment storage in the inland delta section, reaching on average around 1500
499 m³/year/km, indicates that this section continued to act as a sediment storage zone. For the
500 last few centuries, the upper and middle valley experienced greater aggradation which was
501 almost equivalent to all the volume of the others sections added. The total volume of stored
502 sediments was about 63 900 m³/year.

503

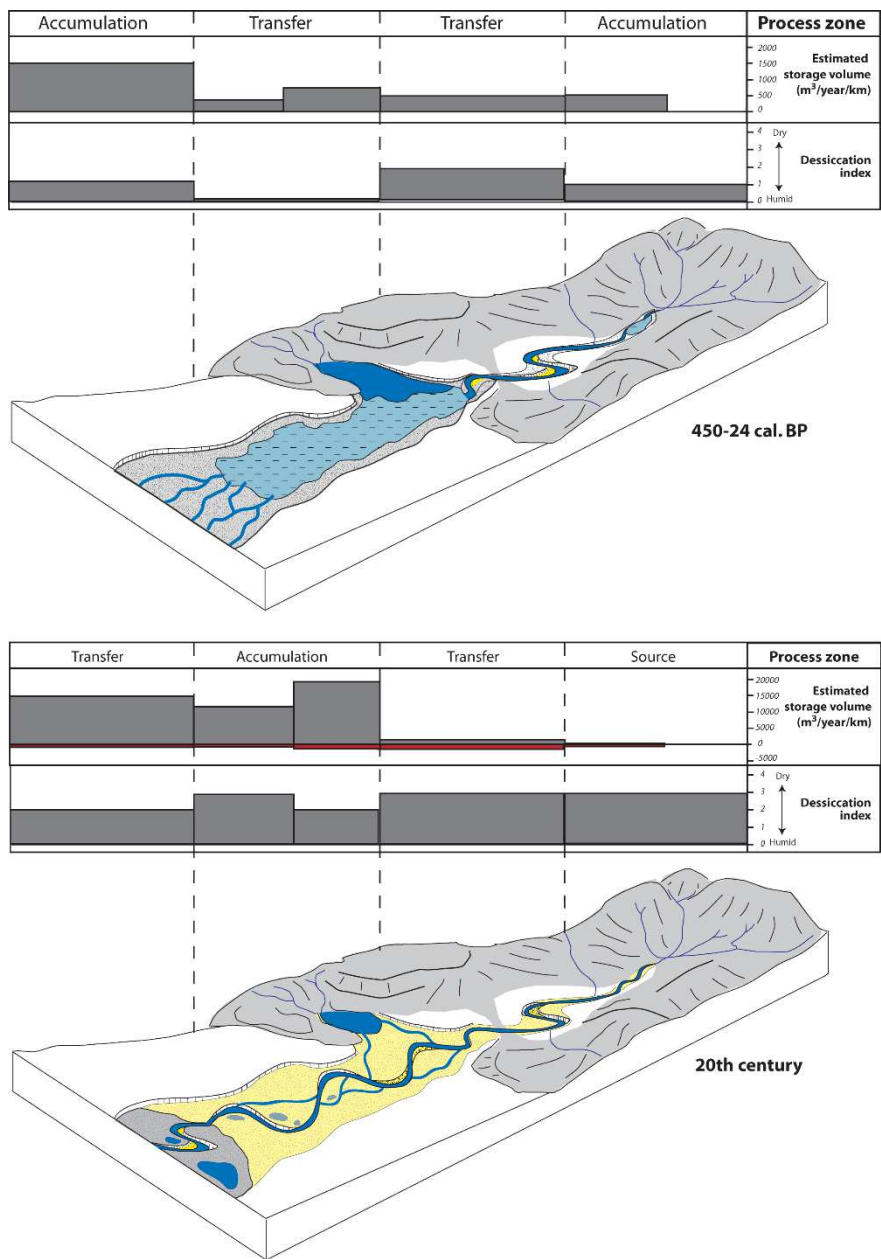


504

505 **Fig. 9.b: Fluvial dynamics reconstruction along the Yamé valley during 1700-**
 506 **450 cal. BP. Sediment storage is indicated for each section by m³ an average of**
 507 **year and km.**

508 During the last decades (**post 1936 CE**), the Yamé River has experienced a new
 509 metamorphosis of fluvial style. A huge incision observed at the valley head reached a
 510 thickness of 12m at Ounjougou (see above). For the rest of the valley, a strong lateral
 511 erosion of river banks occurred. During the year or decades that followed this event, pulsed
 512 sediments were transferred downstream and promoted an aggradation of the valley bottom

513 mainly in the lower valley which acted as a sediment storage zone. This erosion is equivalent
 514 to a volume of 10 million m³. Parallel to this event is a significant aggradation of 596 000
 515 m³/year for the whole valley.

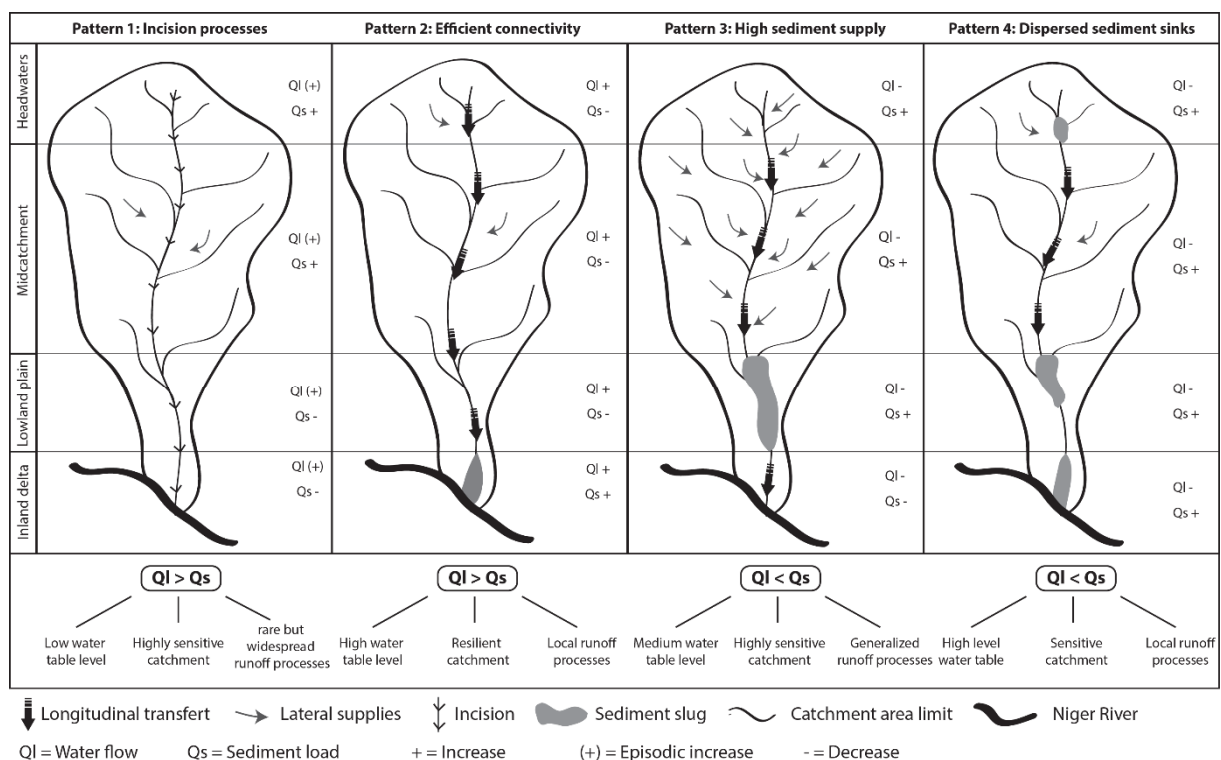


516
 517 **Fig. 9.c: Fluvial dynamics reconstruction along the Yamé valley during 450 cal.**
 518 **BP-20th century. Sediment storage is indicated for each section by m³ an**
 519 **average of year and km.**

520

521 **5. Discussion: Understanding changes in the sediment**
 522 **distribution patterns: which factors and which scales matter?**

523 According to the idealized fluvial system concept by Schumm (1977) sediment storage
 524 increases progressively along the valley floor from source zones in headwaters to
 525 accumulation zones located downstream. Continuity of sediment movement along the fluvial
 526 system reflects the availability of water energy to mobilize sediments (Fryirs et al., 2007;
 527 Fryirs, 2013). Our results show that sometimes the Yamé fluvial system response can be
 528 jerky reflecting a disconnectivity between different compartments of the catchment sediment
 529 cascade. Analysis of the spatio-temporal variability of sediment storage or incision for the
 530 late Holocene has helped to characterize the pattern and processes of sediment movement
 531 within a catchment (e.g. Schumm, 1977; Trimble, 1981; Schumm and Rea, 1995; Fryirs and
 532 Brierley, 2001). In this study, four distinct sediment distribution patterns have been
 533 highlighted during the Late Holocene (Fig. 10). These patterns reveal changes in sediment
 534 and water discharge whose origin may be from external triggers such as climatic events or
 535 oscillations, or from internal changes such as land use, or a combination of the two.

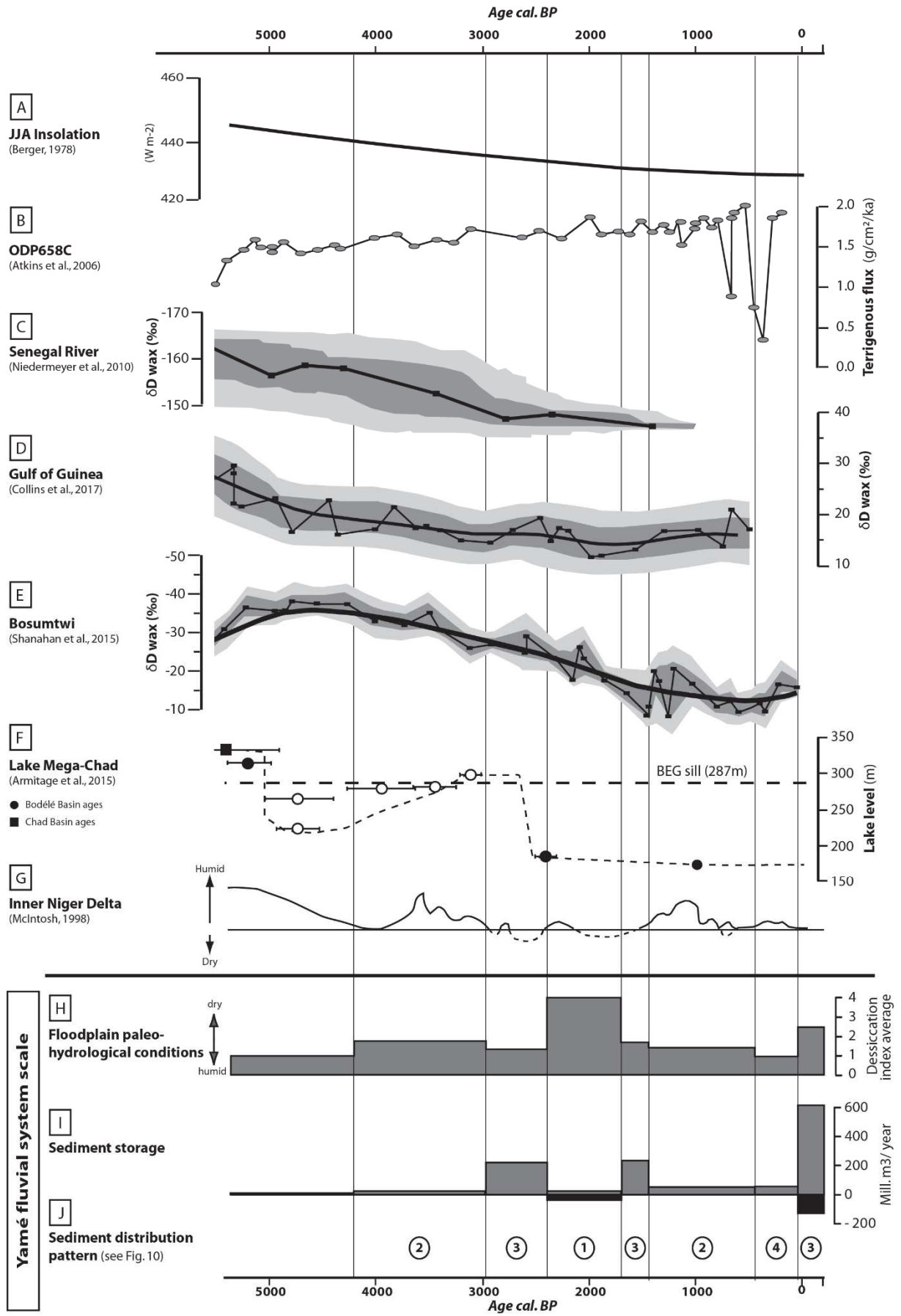


536

537 **Fig. 10: Schematic sediment distribution patterns in the Yamé valley during the**
538 **Late Holocene.**

539

540 In semi-arid catchment areas, because of the high sensitivity of the vegetation and the strong
541 connectivity between slopes and channels, the effects of climatic or anthropogenic changes
542 are particularly rapid (Knighton, 1998; Frankl et al., 2011). To evaluate the sediment and
543 water supplies changes more accurately, we applied to each studied fluvial zone and pattern,
544 the equations of Frankl et al. (2011) based on the concept of Schumm (1977) and Knighton
545 (1998). Channel aggradation (d-) results from an increase in sediment supply (Q_{s+}) and/or a
546 decrease of water flows while channel incision (d+) signals an increase in water flow (QI)
547 and/or a decrease of sediment load (Q_{s-}). A comparison with available palaeoenvironmental
548 datasets from the end of the African Humid period from the region is necessary to discuss
549 the role played by different factors in these morphological adjustments (Fig. 11).



550

551

552 **Fig. 11: Comparison of fluvial record of the Yamé with local regional climatic data**

553 **A.** Mean June-August Insolation at 10°N (Berger, 1978); **B.** Terrigenous flux record from ODP Site
554 685C (Adkins et al., 2006); **C-E.** δD wax from the Senegal River from core GeoB9508-5 (**C.** based on
555 the C_{31} n-alkane; ice-volume and vegetation adjusted - Niedermeyer et al., 2010); The Gulf of Guinea
556 from core GeoB4905-4 (**D.** based on the C_{29} n-alkane; ice-volume and vegetation adjusted - Collins et
557 al., 2017); The Bosumtwi Lake (**E.** based on the C_{31} n-alkane; ice-volume and vegetation adjusted -
558 Shanahan et al., 2015). Shading reflects 66% (dark) and 95% (light) uncertainty bounds. **F.** Lake
559 Mega Chad levels. Point data are from the Bodélé Basin, whereas square ones are from the Chad
560 Basin. Open data points represent Aeolian sediments, which were deposited above the
561 contemporaneous lake level. Closed data points represent shorelines and therefore contemporaneous
562 lake level. The black dashed line indicates lake-level changes while the the horizontal dashed line
563 represents the elevation of the Bahr El Ghazal sill which separates lakes exist in the Chad and
564 Bodelé basin. So lake-level changes below this line represent the Bodelé basin only. **G.** Climatic
565 variations of the Inner Niger delta after McIntosh, 1998. **H-J:** Yamé river data. **H.** Dessication index
566 average reflecting floodplain paleohydrological conditions of the whole valley; **I:** Sum of sediment
567 storage per period for the valley (in mill.m³/year); **J.** Sediment distribution pattern per period.

568

569 **5.1. Intense and widespread incision in the valley during the 2350-1700 cal.**

570 **BP: climate crisis?**

571 This sediment distribution pattern (pattern 1; Fig. 10) is characteristic of a major down cutting
572 of the channel bed occurring ca. 2350-1700 and signifies a hydro-sedimentary crisis (Garnier
573 et al., 2015). This geomorphological adjustment, synchronous for the whole valley, is the
574 result of a dysfunction of the flow-sediment balance and a high sensitivity of the watershed.
575 In particular, it reflects a significant increase in the water supply of the river compared to
576 sediment load ($Q_l > Q_s$). Generally, a rise in water flow compared to sediment supply may
577 originate from increased precipitation and/or dense vegetation cover. But conversely, it can
578 also be linked to the action of consecutive flash floods on a sensitive watershed during an
579 arid period. This latter scenario has been suggested for the Ounjougou's reach (Lespez et
580 al., 2011) and has already been observed in other semi-arid regions (Berger et al., 2012) and
581 also more recently in the Sahelo-Sudanian region during the 70-80's. Despite a decrease in
582 rainfall, studies suggest an increase of flow coefficients (Valentin et al., 2004; Garnier et al.,

583 2015). During droughts, sporadic rains result in an increase of hortonian runoff because of
584 the low infiltration capacity of the soils. The decline in vegetation cover promotes soil crust
585 formation and makes these soils more sensitive to an extreme climatic event (Casenave and
586 Valentin, 1992; Wilcox et al., 1998). This hypothesis of a more arid oscillation is supported in
587 the lower valley by the drying up of the Bandiougou's Lake which became a swampy area.
588 In West Africa, some studies argue that this period was arid (Lézine., 1989, 2011; Shanahan
589 et al., 2006; Armitage et al., 2015). A significant decrease of flow rates of the Senegal River
590 is observed between 2500-2200 cal. BP (Bouimetarhan et al., 2009). Between ca. 2200 and
591 2100 cal yr BP, a rapid increase in sedimentation rates and important proxies percentage
592 fluctuations (fern spores, pollen, dinocysts, etc.) suggests high magnitude river discharge
593 which can be interpreted as the result of episodic flash-flood events of the Senegal River
594 (Bouimetarhan et al., 2009). This period is also associated with a greater peak in terrigenous
595 fluxes indicating more arid conditions (Fig. 11B; Adkins et al., 2006). In the Middle Niger an
596 arid phase called the "Big Dry" is recorded (McIntosh, 1998; Makaske, 1998) while the Inland
597 Niger Delta is subject to a long period of drought (Makaske et al., 2007). Water levels from
598 Chad Lake fell after 3 ka. BP. On 2400 cal. BP, it reached the sill of 287m, which is the limit
599 to feed northward the Bodelé basin by overflow through the Bahr el Ghazal (Fig.11F;
600 Armitage et al., 2015). According to Maley and Vernet (2015) a significant erosive phase
601 occurred south of the Sahara between 2400-1800 cal. BP. Indeed, an incision of several tens
602 of meters is observed along the Bahr el Ghazal even to the Congo basin, with the
603 identification of coarse deposits associated with erosive dynamics (Maley, 2010).
604 Nevertheless, the archives from the current Sudano-Guinean zone show no change in the
605 vegetation cover for this period, with palynological and phytoliths records of the Sudano-
606 Sahelian zone indicating a permanent opening of the vegetation (Maley, 1981; Lézine, 1988,
607 1989; Alexandre et al., 1997). Ngomanda et al., (2009) demonstrate a significant increase in
608 Poaceae around 2,500 years old. BP. Gulf Guinea δD_{wax} record are the lowest during this
609 period suggesting a decrease in antecedent rainfall (Fig.11D; Collins et al., 2017).
610 Palaeoenvironmental studies concur that this period was determinant in the history of the

611 Holocene in West Africa. Archaeological studies also testify to the importance of population
612 dynamics during this dry period, particularly in wetland areas such as the Inner Niger Delta,
613 the Senegal delta (McIntosh and McIntosh, 1983; McIntosh, 1999, 2005; Mayor et al., 2005)
614 or local refuge areas with permanent water sources (Garnier et al., 2015).

615 **5.2. Efficient connectivity within the catchment basin reflecting humid phases** 616 **(4200-2900 cal. BP and 1400-450 cal. BP)**

617 Two periods testify to an efficient sediment conveyor belt with a sediment wave that operated
618 from headwaters to the Inland Niger Delta (Pattern 2; Fig. 10). This fluvial pattern suggests
619 that the competence and capacity of flow are sufficient to transport sediments along the
620 valley to the storage basin downstream. Alluvial records of these time slices reflect the same
621 geomorphological conditions. Desiccation indexes around 1.8 and 1.25 on average attest to
622 the presence of a moderate to high water table in the whole valley (Fig. 11H). However, the
623 most conspicuous feature of this fluvial system pattern is the weakness of the sediment
624 supply. The storage record for both of these periods is the lowest of the Late Holocene with
625 <500 m³/yr/km on average for the whole basin. Indeed, the combination of moderate and
626 stable water flow is sufficient to transfer sediment and relatively low sediment supply could
627 explain the good connectivity between landscapes units, from headwater to accumulation
628 zone, downstream.

629 The weakness of sediment supply could also have been promoted by the presence of dense
630 vegetation cover, sufficient to protect soils from runoff. This interpretation is in line with
631 regional data that confirm the presence of a relatively humid period for the first period.
632 Despite the fact that the 5th millennium is often described as the termination of the African
633 Humid Period (Gasse, 2000; deMenocal et al., 2000; Salzmann et al., 2002; Lézine et al.,
634 2005; Armitage et al., 2015; Collins et al., 2017), studies indicate some spatio-temporal
635 variability with the identification of a new wet period during the 4th millennium BP. Lake Chad
636 is lived his last transgression around 3000 cal. BP (Leblanc et al., 2006; Maley and Vernet,
637 2015; Armitage et al., 2015; Fig. 11F) while more locally, the level of the Niger, after a

638 significant regression around 4000 cal. BP, became higher until ca. 2400 cal. BP in the
639 Inland Niger Delta (McIntosh, 1998, 2005; Fig. 11G). The crater lake Bosumtwi δD_{wax}
640 records testify to a return to wet conditions around 5.5 ka and then a termination of the
641 African Humid Period at ~ 3.5 ka (Fig. 11E; Shanahan et al., 2015). More generally, Lézine et
642 al. (2011) compiled the palaeohydrological proxies in lacustrine, fluvial or palustrine deposits
643 and showed that the Sahel had a period of relative humidity between 3500 and 2500 cal BP.
644 On the other hand, it appears very different for the 1400-450 cal. BP period. Locally, many
645 colluvial deposits have been observed on the sandstone plateau suggesting an increase in
646 soil sensitivity (Fig. 9.b). Some regional environmental data postulate about a humid climate.
647 After an arid period, an increase in water level is recorded between 1400-1000 cal. BP in the
648 Inland Niger Delta (Fig. 11G; McIntosh, 1998) which then became more variable (Mayor et
649 al., 2005). Nearby, in Saouga (Burkina Faso), this short climatic improvement was marked by
650 the migration of various Sudanese plant taxa in a Sahelian floristic context (Neumann et al.,
651 1998). Historical data also points to a more humid period around 900-1000 cal. BP (Reichelt
652 et al., 1992). However, this short climatic pulse could have a local extent because further
653 away other data testify to a continuous trend towards aridification. Indeed, this was confirmed
654 by a regression of the Lake Chad level (Maley, 1981; Leblanc et al., 2006; Armitage et al.,
655 2015) and stronger aeolian activity (Makaske, 1998; Adkins et al., 2006).
656 Despite a different environmental context, the good connectivity suggests that changes in the
657 vegetation cover and in the catchment area sensibility are not the dominant driving factor and
658 that climate was sufficiently wet to produce flows available to transfer sediment throughout
659 the valley.

660 **5.3. An increase in sediment supply: a result of a degraded catchment?** 661 **(2900-2350 cal. BP; 1700-1400 cal. BP; 20th century)**

662 The third sediment distribution pattern reveals a sediment wave from upstream with a
663 substantial aggradation of sandy sediments downstream (Fig. 10). The volume of sediment
664 storage in the low valley ranges between 8200 and 9300 m³/yr/km for the two older periods

665 and more than 17000 m³/yr/km for the 20th century. The flow is inefficient to transport
666 sediments that are trapped at the entrance into the lower valley that can be characterized by
667 a decrease of the longitudinal slope and energy (Fig. 1). This geomorphic adjustment
668 resulted in floodplain width expansion. This sediment slug acted as an obstacle to
669 longitudinal sediment transfer altering the water-sediment balance with an increase of
670 sediment load ($Q_s > Q_l$). This reflects a highly sensitive catchment originating from climate
671 and/or vegetation cover changes. A decline of vegetation cover may induce intensified
672 erosion on hillslopes and increased sediment delivery downstream.

673 For the older period (2900-2400 cal. BP), the geomorphological data signifies a relatively wet
674 period with a desiccation index reaching 1.3 on average for the whole valley. However, this
675 desiccation index can also be explained by the sudden aggradation of the valley floor in the
676 lower valley creating a vast spreading watery area with some remaining small pools.. This
677 also indicates a local geomorphological adjustment. Moreover, first colluvial deposits have
678 been observed upstream and this suggests an increase in soil erosion. On a regional scale,
679 some studies demonstrate a trend towards aridification for this period (Breuning and
680 Neumann, 2002; Mayor et al., 2005). Re-activation of a dune system was recorded during
681 2700-2500 cal. BP in the Gourma (Stokes et al., 2004), in the Inland Niger Delta (Makaske,
682 1998), in Mauritania (Hanebuth and Lantsch, 2008) and further north at Ounianga, north of
683 Chad (Kröpelin et al., 2008). Vegetation data at Oursi dated to ca. 3000 cal. BP suggest a
684 more arid period (Ballouche and Neumann, 1995). Other analyses conducted on marine
685 cores retrieved off the Senegal River mouth reveal increased runoff from the Senegal River
686 but was related however by authors to higher monsoonal precipitation (Bouimetarhan et al.,
687 2009; Nizou et al., 2010). Niedermeyer et al. (2010) studying the δD record from a marine
688 sediment core from the continental slope off Senegal showed a strong decrease in their
689 results suggesting aridification during this period (Fig.11C).

690 Archaeological data highlight a possible role played by human activities in this significant
691 increase in sediment delivery. Even if signs of agriculture are recorded at Ounjougou around
692 circa 3900-3400 cal. BP (Ozainne et al., 2009; Garnier et al., 2013), it seems that this activity

693 was even more intense over a millennium later, and contributed towards accelerating soil
694 erosion. [Eichhorn and Neumann \(2013\)](#) point to an openness in the vegetation cover and a
695 diversification of habitats maybe promoted by agricultural practices. Hence, this period
696 follows an increase in the archaeological record of artifacts which confirms the presence of
697 farmers in the region, particularly on the sandstone plateau ([Ozainne, 2013](#); [Ozainne et al.,](#)
698 [2009](#)). Thus, drier climatic conditions associated with an increase in agriculture practices on
699 the sandstone plateau would have probably favored high runoff on watershed slopes.

700 The second period (1700-1400 cal BP) is specific because it is the lag time or recovery
701 period after an arid period (2350-1700 cal. BP). The rise of precipitation and the reactivation
702 of the water flows resulted in an increase in sediment supply and water discharge. Sediment
703 records at Bandiougou show an extension of the lake and wetlands and suggest the
704 possibility of a wetter climate. This is in agreement with [McIntosh \(1998, 2005\)](#), who
705 suggests an increase in the water table in the Inland Niger Delta ([Fig.11G](#)). A rise in the
706 δD_{wax} record of Gulf Guinean indicates as well an increase in past precipitation ([Collins et](#)
707 [al., 2017D](#)). The recovery of more humid conditions would have been favorable to soil
708 stability but we suggest that human activities would have certainly accelerated soil
709 degradation. Local archaeological data points towards an expansion of human occupation
710 and agro-pastoral activities during these centuries ([Mayor et al., 2005, 2014](#); [Mayor, 2011](#);
711 [Huysecom et al., 2009](#); [Ozainne et al., 2009](#); [Ozainne, 2013](#)) while other
712 palaeoenvironmental data suggest the development of a sedentary lifestyle in West Africa
713 leading to the expansion of cultivated areas ([Höhn and Neumann, 2012](#); [Ozainne et al.,](#)
714 [2014](#); [Davidoux et al., 2018](#); [Stern et al., in press](#)). Land clearance and agricultural activities
715 associated with hydrological reactivation created a direct impact on surface runoff and soils
716 erosion. However, the frequency and intensity of flood flows were not sufficient to transfer all
717 these sediments to the Inland Niger Delta.

718 More recently, the Yamé valley was subject to a cut and fill hydro-sedimentary pattern. At
719 Ounjougou, this strong incision, around 10m in the Quaternary deposits, can be related to

720 the oral tradition and dating back to 1936 (Rasse et al., 2006). According to the
721 chronostratigraphy, the incision of around a few meters observed in the whole valley,
722 occurred during the same period or slightly after (post 24 cal. BP). Despite the shortness of
723 the period, the sediment volume stored is significant (49 million m³) and testifies to a high
724 denudation rate and an increase in runoff coefficients. This intense degradation of vegetation
725 cover might be the result of an increase of aridification as hinted at by the desiccation index
726 reaching the highest level (2.7) since the beginning of the Late Holocene but also an
727 increase promoted by human pressure. The local meteorological data point towards more
728 arid conditions not seen since the second part of the 20th century (Garnier et al., 2014). In
729 addition, Mayor (2005) noted an increase in the demographic pressure from the 18th century
730 CE resulting from a new wave of migration from the populations of Mandé (South of Mali) to
731 the Dogon Country. Most of the current villages were settled during this century. In Sahel, the
732 second half of the 20th century is also characterized by one of the world's highest population
733 growth episodes. Leblanc et al. (2008) show that 80% of their study area (500 km²) in SW
734 Niger had been cleared between 1950 and 1992. First, to open up new areas for agricultural
735 use but also for firewood supplies.

736 Despite different environmental conditions, the combination of both of these external and
737 internal triggers played a role in this major geomorphological event. For both time periods,
738 2900-2400 cal. BP and the 20th century, the huge increase in sediment supply is the result of
739 climate aridification associated with an increase of anthropogenic impact on the Yamé valley
740 catchment. The fluvial response of the 1700-1400 cal. BP period is more complex because
741 geomorphological inheritance of the preceding arid period and increases in human
742 populations and agricultural practices must be taken into consideration. The aridification of
743 the climate over more than seven centuries created a higher sensitivity of the landscapes
744 with the opening of the vegetation and degradation of the soils. A more humid climate
745 conducted to the reactivation of hydrological processes as well as the reoccupation by
746 human populations in the Yamé valley increased substantially the runoff processes and
747 sediment delivery.

748 **5.4. Disperse sediment sinks : local adjustment to human disturbance and**
749 **climatic pulse (450-24 cal. BP)**

750 Sedimentary records of the last centuries (450-24 cal. BP) are representative of the last
751 sediment delivery pattern (Fig. 10). This pattern is quite similar to the first one with a
752 sediment slug processing from the sandstone plateau to the Inland Niger Delta. However,
753 except in the middle valley which acted as a sediment transfer zone, some sections reveal
754 the development of wetland environments throughout the valley, which acted as a storage
755 area. The sedimentary facies and the desiccation index, which decreased to 1, suggest a
756 rise in the water table level and increase in precipitation. According to McIntosh (1998), a wet
757 phase occurred between 500-200 cal. BP in the Inland Niger Delta (Fig. 11G) and from 400
758 cal. BP to the beginning of the 20th century in Lake Chad (Maley, 1981). Terrigenous fluxes in
759 sediments from the marine core ODP Site685C off Cape Blanc show a large drop (Fig.11B;
760 Factor of 1.5-2.0 vs. factor of <1) at the beginning of this period suggesting important
761 changes in vegetation cover and/or precipitation (Adkins et al., 2006; McGee et al., 2013).
762 On a global scale, this period may be correlated with the last rapid climate change identified
763 by Mayewski et al. (2004) and Wanner et al. (2011). It also corresponds in Europe to the
764 'Little Ice Age' which resulted in wetter conditions in the tropics ("Cool poles, wet tropics",
765 Mayewski et al., 2004). Despite this well-recorded rapid climatic change across the world,
766 studies reveal that this event has not been yet observed in West Africa. We can also
767 suppose that the local swamps promoted by the expansion of the sediment slugs which
768 acted as plugs to longitudinal sediment movement along channels and creating further vast
769 swampy areas. Indeed, archaeological data is numerous for this period (Mayor et al., 2005).
770 For example, the Dogon settlement developed during this time period and increased the
771 impact of human activities on the environment in this region. Increases in sediment supplies
772 and the local sediment delivery may have been plugged in the valley floor according to the
773 topography features and the climatic conditions. Thus, these local swamps lasting several

774 decades to a century in large unconfined reach formed due to climatic oscillations and
775 sediment supply increases.

776

777 **6. Conclusion**

778 Just as Holocene fluvial system responses have already been well studied in temperate and
779 Mediterranean zones (e.g: [Faust and Wolf, 2017](#); [Verstraeten et al., 2017](#); [Brown et al.,](#)
780 [2018](#)), research conducted on medium size tropical rivers remain scarce, especially in Africa.
781 The study of the Late Holocene sedimentary records of the Yamé valley provide new
782 information about climatic and anthropogenic changes for a region and period poorly studied
783 to date. Thus, the analyses of sediment archives for seven reaches distributed along the
784 entire course of the 137km of the Yamé valley (Mali) is the first study to attempt to
785 reconstruct the fluvial system operating from the source to the accumulation zone during the
786 Holocene in tropical West Africa. This study has attempted to address questions of time and
787 scale which are crucial to the understanding of fluvial archives and to interpreting themes in
788 terms of system responses to different controls (e.g. [Schumm, 1991](#); [Harvey, 2002](#)). This
789 study demonstrates the possibility for each time slice and river reach (1) to reconstruct the
790 fluvial style and processes and (2) to estimate the sediment storage volume reflecting
791 sediment and water delivery changes whose origin may be from external (climatic events) or
792 local (land use, etc.) controls or a combination of both. The results obtained from this
793 research highlight the role of the wet oscillation (4200-2900 cal. BP, 450-24 cal. BP) and arid
794 period (2350-1700 cal. BP). This study confirms that climatic factors play a crucial role in the
795 timing of the fluvial system changes in semi-arid and tropical rivers (e.g. [Thomas, 2008](#);
796 [Macklin et al., 2015](#); [Faust and Wolf, 2017](#)) while human disturbance appears as a
797 secondary driver due to the high sensitivity of the environment to climate variability in such
798 areas. If we can assume that human practices have certainly intensified runoff processes
799 during the Late Holocene, it remains difficult to disentangle and quantify the role played by

800 human activities. Nevertheless, we observe an intensification in erosion and sediment
801 supplies, even during more arid periods. It can be interpreted as an increase in human
802 pressure on the environment. This is the case during the 2900-2350 cal. BP period
803 corresponding to the beginning of the agro-pastoral activities development but also more
804 recently, during the demographic explosion of the 20th century generating an extension and
805 intensification of agricultural practices (Garnier et al., 2014).

806 This study also highlights the role of sediment and geomorphic legacies in the response of
807 the river system to environmental changes and emphasizes the necessity for understanding
808 the trajectory of the fluvial system for interpreting the fluvial archive. For the 1700-1400 cal.
809 BP period, fluvial archives record huge sediment supplies which can be explained mainly by
810 the reactivation of both hydrological processes (on slopes and channels) and human
811 occupation after an intense and long arid event. Thus, this record appears as a complex and
812 strong response to long-term change in the environment not only proportional to the intensity
813 of climate change but also subject to the state of the environment and fluvial system before
814 this change occurred. On the other hand, the last sediment delivery pattern (450-24 cal. BP)
815 testifies to the strong reactivity of the fluvial system with local fluvial adjustments to human
816 disturbance. Fluvial archives demonstrate that for many reaches disperse sediment sinks
817 result both from the combination of local intensification of colluvial processes and of global
818 climatic change with wet phase occurring at the regional scale. These factors also have to be
819 considered for the management and prediction of fluvial system changes due to global and
820 local land use changes.

821 To conclude, the results from this study highlight the need for researchers to undertake new
822 palaeoenvironmental analyses in order to better capture and characterize the vegetation
823 cover changes. Certainly, these analyses will provide new information on human-
824 environment interactions and enable researchers to discuss, more accurately, the role of
825 these factors in changes in the fluvial landscapes during the Late Holocene. Furthermore,
826 this kind of global fluvial system study should be developed South of the Sahara in order to

827 make further comparisons useful to understand the role of geographical contexts and local
828 controls vs. global changes in the river changes in Africa.

829 **Acknowledgements**

830 We would like to thank our Malian colleagues for support work in the field and the members
831 of the project 'Human populations and paleoenvironment in West Africa' especially Eric
832 Huysecom. We are particularly grateful to Aziz Ballouche for helping coring at Sampara, to
833 Daniel Delahaye for judicious advices and Charlene Murphy for language editing. The
834 authors are indebted to the anonymous reviewers for their very helpful comments.

835 **Funding**

836 This study is part of the ANR-DFG project 'Archéologie du paysage en Pays Dogon' (APPD)
837 and of the PhD Dissertation of Aline Garnier funded by Région Basse-Normandie.

838 **References**

- 839 Adkins, J., deMenocal, P., Eshel, G., 2006. The "African humid period" and the record of
840 marine upwelling from excess ^{230}Th in Ocean Drilling Program Hole 658C.
841 *Paleoceanography*, 21 (4). PA4203 <https://doi.org/10.1029/2005PA001200>
- 842 Alexandre, A., Meunier, J.D., Lézine, A.M., Vincens, A., Schwartz, D., 1997. Phytoliths:
843 indicators of grassland dynamics during the late Holocene in intertropical Africa.
844 *Palaeogeography, Palaeoclimatology, Palaeoecology*. 136 (1), 213-229.
845 [https://doi.org/10.1016/S0031-0182\(97\)00089-8](https://doi.org/10.1016/S0031-0182(97)00089-8)
- 846 Armitage, S.J., Bristow, C.S., Drake, N. A., 2015. West African monsoon dynamics inferred
847 from abrupt fluctuations of Lake Mega-Chad. *Proceedings of the National Academy of*
848 *Sciences*, 112 (28), 8543-8548. <https://doi.org/10.1073/pnas.1417655112>

849 Ballouche, A., Neumann, K., 1995. A new contribution to the Holocene vegetation history of
850 the West African Sahel: pollen from Oursi, Burkina Faso and charcoal from three sites in
851 northeast Nigeria. *Vegetation History and Archaeobotany*. 4, 31-39.

852 Berger, J.-F., Bravard, J.-P., Purdue, L., Benoist, A., Mouton, M., Braemer, F., 2012. Rivers
853 of the Hadramawt watershed (Yemen) during the Holocene: Clues of late functioning.
854 *Quaternary International*. 266, 142-161. <https://doi.org/10.1016/j.quaint.2011.10.037>

855 Bouimetarhan, I., Dupont, L.M., Schefufl, E., Mollenhauer, G., Mulitza, S., Zonneveld, K.,
856 2009. Palynological evidence for climatic and oceanic variability off NW Africa during the late
857 Holocene. *Quaternary Research*. 72, 188-197. <https://doi.org/10.1016/j.yqres.2009.05.003>

858 Bravard, J.-P., Peiry, J.-L. 1999. The CM pattern as a tool for the classification of alluvial
859 suites and floodplains along the river continuum. Geological Society, London, Special
860 Publications. 163(1), 259-268. <https://doi.org/10.1144/GSL.SP.1999.163.01.20>

861 Breunig, P., Neumann, K., 2002. From hunters and gatherers to food producers: New
862 archaeological and archaeobotanical evidence from the West African Sahel. In: Hassan, F.
863 (Eds.), *Droughts, Food and Culture. Ecological change and food security in Africa's later*
864 *Prehistory*. New York: Kluwer Academic Plenum publishers, pp. 123-155.
865 https://doi.org/10.1007/0-306-47547-2_9

866 Brown, A.G., Lespez, L., Sear, D.A., Macaire, J.-J., Houben, P., Klimek, K., Brazier, R.E.,
867 Van Oost, K., Pears, B., 2018. Natural vs anthropogenic streams in Europe: History, ecology
868 and implications for restoration, river-rewilding and riverine ecosystem services, *Earth*
869 *Science Reviews*. In Press. <https://doi.org/10.1016/j.earscirev.2018.02.001>

870 Casenave, A., Valentin, C., 1992. A runoff capability classification system based on surface
871 features criteria in semi-arid areas of West Africa. *Journal of Hydrology*. 130 (1-4), 231-249.
872 [https://doi.org/10.1016/0022-1694\(92\)90112-9](https://doi.org/10.1016/0022-1694(92)90112-9)

873 Collins, J.A., Prange, M., Caley, T., Gimeno, L., Beckmann, B., Mulitza, S., Skonieczny, C.,
874 Roche, D., Schefuß, E., 2017. Rapid termination of the African Humid Period triggered by
875 northern high-latitude cooling. *Nature Communications*. 8(1), 1372.
876 <https://doi.org/10.1038/s41467-017-01454-y>

877 Davidoux, S., Lespez, L., Garnier, A., Rasse, M., Lebrun, B., Hajdas, I., Tribolo, C.,
878 Huysecom, E. 2018. Les fluctuations environnementales des deux derniers millénaires en
879 Afrique de l'Ouest: premiers résultats de l'étude des terrasses alluviales du ravin de
880 Sansandé (vallée de la Falémé, Sénégal oriental). *Géomorphologie: relief, processus,*
881 *environnement.* 24(3), 237-255.
882 <http://doi.org/10.4000/geomorphologie.12484>

883 deMenocal, P., Ortiz, J., Guilderson, T., Adkins, J., Sarnthein, M., Baker, L., Yarusinsky, M.,
884 2000. Abrupt onset and termination of the African Humid Period: rapid climate responses to
885 gradual insolation forcing. *Quaternary Science Reviews.* 19, 347-361.
886 [https://doi.org/10.1016/S0277-3791\(99\)00081-5](https://doi.org/10.1016/S0277-3791(99)00081-5)

887 Eichhorn, B., Neumann, K., 2013. Holocene vegetation change and land use at Ounjougou,
888 (Mali). In: Stevens, C., Nixon, S., Murray, M.A., Fuller, D.Q. (Eds.), *African Flora, Past*
889 *Cultures and Archaeobotany.* Left Coast Press, Walnut Creek, pp. 83-96.

890 Eichhorn, B., Neumann, K., Garnier, A., 2010. Seed phytoliths in West African
891 Commelinaceae and their potential for palaeoecological studies. *Palaeogeography,*
892 *Palaeoclimatology, Palaeoecology.* 298, 300-310.
893 <https://doi.org/10.1016/j.palaeo.2010.10.004>

894 Faust, D., Wolf, D., 2017. Interpreting drivers of change in fluvial archives of the Western
895 Mediterranean-A critical view. *Earth-Science Reviews.* 174, 53-83.
896 <https://doi.org/10.1016/j.earscirev.2017.09.011>

897 Frankl, A., Nyssen, J., De Dapper, M., Haile, M., Billi, P., Munro, R.N; Deckers, J; Poesen, J.,
898 2011. Linking long-term gully and river channel dynamics to environmental change using
899 repeat photography (Northern Ethiopia). *Geomorphology.* 129 (3-4), 238-251.
900 <https://doi.org/10.1016/j.geomorph.2011.02.018>

901 Fryirs, K., 2013. (Dis) Connectivity in catchment sediment cascades: a fresh look at the
902 sediment delivery problem. *Earth Surface Processes and Landforms.* 38(1), 30-46.
903 <https://doi.org/10.1002/esp.3242>

904 Fryirs, K., Brierley, G.J., 2001. Variability in sediment delivery and storage along river
905 courses in Bega catchment, NSW, Australia: implications for geomorphic river recovery.
906 *Geomorphology*. 38 (3-4), 237-265. [https://doi.org/10.1016/S0169-555X\(00\)00093-3](https://doi.org/10.1016/S0169-555X(00)00093-3)

907 Fryirs, K.A., Brierley, G.J., Preston, N.J., Kasai, M., 2007. Buffers, barriers and blankets: the
908 (dis) connectivity of catchment-scale sediment cascades. *Catena*. 70 (1), 49-67.
909 <https://doi.org/10.1016/j.catena.2006.07.007>

910 Garnier, A., Neumann, K., Eichhorn, B., Lespez, L., 2013. Phytolith taphonomy in the middle-
911 to late-Holocene fluvial sediments of Ounjougou (Mali, West Africa). *The Holocene*. 23, 416-
912 431. <http://dx.doi.org/10.1177/0959683612463102>

913 Garnier, A., Dufour, S., Lespez, L., Caillault, S., Delahaye, D., 2014. Analyse spatio-
914 temporelle de la dynamique fluviale d'un cours d'eau sahélo-soudanien entre 1967 et 2007 :
915 le cas du Yamé au Pays Dogon (Mali, Afrique de l'Ouest). *Revue Internationale de*
916 *Géomatique*. 24 (3), 279-306. <http://dx.doi.org/10.3166/rig.24.279-306>

917 Garnier, A., Lespez, L., Ozainne, S., Ballouche, A., Mayor, A., Le Drézen, Y. Rasse, M.,
918 Huysecom, E., 2015. L'incision généralisée de la vallée du Yamé (Mali) entre 2 350 et 1 700
919 ans cal. BP: quelle signification paléoenvironnementale et archéologique?. *Quaternaire*.
920 26(1), 49-66. <https://doi.org/10.4000/quaternaire.7155>

921 **Garnier, A.**, Eichhorn, B., Robion-Brunner, C. 2018. Impact de l'activité métallurgique au
922 cours du dernier millénaire sur un système fluvial soudano-guinéen. Étude multi-proxy des
923 archives sédimentaires de la vallée du Tatré (pays bassar, Togo). *Géomorphologie : relief,*
924 *processus, environnement*, 24, 3, 257-276. <http://doi.org/10.4000/geomorphologie.12446>

925 Gasse, F., 2000. Hydrological changes in the African tropics since the Last Glacial
926 Maximum. *Quaternary science reviews*. 19, 189-211. [https://doi.org/10.1016/S0277-3791\(99\)00061-X](https://doi.org/10.1016/S0277-3791(99)00061-X)

928 Gumnior, M., 2008. Some new insights on fluvial dynamics and Holocene landscape
929 evolution in the Nigerian Chad Basin. *Zeitschrift für Geomorphologie*. 52, 17-30.
930 <https://doi.org/10.1127/0372-8854/2008/0052-0017>

931 Gumnior, M., Thiemeyer, H., 2003. Holocene fluvial dynamics in the NE Nigerian Savanna:
932 some preliminary interpretations. *Quaternary International*. 111, 51-58.
933 [https://doi.org/10.1016/S1040-6182\(03\)00014-4](https://doi.org/10.1016/S1040-6182(03)00014-4)

934 Hanebuth, T.J.J, Lantsch, H., 2008. A Late Quaternary sedimentary shelf system under
935 hyperarid conditions: Unravelling climatic, oceanographic and sea-level controls (Golfe
936 d'Arguin, Mauritania, NW Africa). *Marine Geology*. 256, 77 –89.
937 <https://doi.org/10.1016/j.margeo.2008.10.001>

938 Harvey, A.M., 2002. Effective timescales of coupling within fluvial systems. *Geomorphology*.
939 44, 175–201. [https://doi.org/10.1016/S0169-555X\(01\)00174-X](https://doi.org/10.1016/S0169-555X(01)00174-X)

940 Hély, C., Braconnot, P., Watrin, J., Zheng, W., 2009. Climate and vegetation: simulating the
941 African humid period. *Comptes Rendus Geoscience*. 341(8-9), 671-688.
942 <https://doi.org/10.1016/j.crte.2009.07.002>

943 Huysecom, E., 2002. Palaeoenvironment and human population in West Africa: an
944 international research project in Mali. *Antiquity*. 76, 335-336.
945 <https://doi.org/10.1017/S0003598X00090396>

946 Huysecom, E., Ozainne, S., Raeli, F., Ballouche, A., Rasse, M., Stokes, S., 2004. Ounjougou
947 (Mali): A history of Holocene settlement at the southern edge of the Sahara. *Antiquity*. 78
948 (301), 579-593.

949 Huysecom, E., Rasse, M., Lespez, L., Neumann, K., Fahmy, A., Ballouche, A., Ozainne, S.,
950 Maggetti, M., Tribolo, C., Soriano, S., 2009. The emergence of pottery in Africa during the
951 10th millennium cal BC: new evidence from Ounjougou (Mali). *Antiquity*. 83 (322), 905-917.
952 <https://doi.org/10.1017/S0003598X00099245>

953 Höhn, A., Neumann, K., 2012. Shifting cultivation and the development of a cultural
954 landscape during the Iron Age (0-1500 AD) in the northern Sahel of Burkina-Faso, West
955 Africa: Insights from archaeological charcoal. *Quaternary International*. 249, 72-83.
956 <https://doi.org/10.1016/j.quaint.2011.04.012>

957 Knighton, A.D., 1998. *Fluvial forms and processes*. Edward Arnold, London.

958 Knox, J.C., 1983. Responses of river systems to Holocene climates. Late quaternary
959 environments of the United States. 2, 26-41.

960 Kröpelin, S., Verschuren, D., Lézine, A.M., Eggermont, H., Cocquyt, C., Francus, P., Cazet,
961 J.P., Fagot, M., Rumes, B., Russell, J.M., Darius, F., Conley, D.J., Schuster, M., von
962 Suchodoletz, H., Engstrom, D.R., 2008. Climate-driven ecosystem succession in the Sahara:
963 The past 6000 years. *Science*. 320, 765-768. <https://doi.org/10.1126/science.1154913>

964 Le Drézen, Y., Garnier, A., Ballouche, A., Lespez, L., 2014. Dix ans de recherches
965 géoarchéologiques au Pays dogon (Mali, Afrique de l'Ouest). Focus sur des méthodologies
966 récentes adaptées aux milieux fluvio-palustres africains, in Arnaud-Fassetta, G., Carcaud, N.
967 (Eds), *Geoarchaeology*. CNRS Press, Paris, pp. 23-34.

968 Le Drézen, Y., Lespez, L., Rasse, M., Garnier, A., Coutard, S., Huysecom, E., Ballouche, A.,
969 2010. Hydrosedimentary records and Holocene environmental dynamics in the Yamé Valley
970 (Mali, Sudano-Sahelian West Africa). *Comptes Rendus Geoscience*. 342, 244-252.
971 <https://doi.org/10.1016/j.crte.2009.12.005>

972 Leblanc, M., Favreau, G., Maley, J., Nazoumou, Y., Leduc, C., Stagnitti, F., Van Oevelen, P.
973 J., Delclaux, F., & Lemoalle, J., 2006. Reconstruction of Megalake Chad using February
974 2000 Shuttle Radar Topographic Mission data. *Palaeogeography Palaeoclimatology*
975 *Palaeoecology*. 239, 16–27. <https://doi.org/10.1016/j.palaeo.2006.01.003>

976 Leblanc, M.J., Favreau, G., Massuel, S., Tweed, S.O., Loireau, M., Cappelaere, B., 2008.
977 Land clearance and hydrological change in the Sahel: SW Niger. *Global and Planetary*
978 *Change*. 61 (3-4), 135-150. <https://doi.org/10.1016/j.gloplacha.2007.08.011>

979 Lespez, L., Rasse, M., Le Drézen, Y., Tribolo, C., Huysecom, E., Ballouche, A., 2008.
980 L'évolution hydromorphologique de la vallée du Yamé (Pays Dogon, Mali): signal climatique
981 et hydrosystème continental en Afrique de l'Ouest entre 50 et 4 ka cal. BP. *Géomorphologie:*
982 *relief, processus, environnement*. 3, 170-185. <https://doi.org/10.4000/geomorphologie.7053>

983 Lespez, L., Le Drézen, Y., Garnier, A., Rasse, M., Eichhorn, B., Ozainne, S., Ballouche, A.,
984 Neumann, K., Huysecom, E., 2011. High-resolution fluvial records of Holocene

985 environmental changes in the Sahel: the Yamé River at Ounjougou (Mali, West Africa).
986 Quaternary Science Reviews. 30, 737-756. <https://doi.org/10.1016/j.quascirev.2010.12.021>

987 Lézine, A.-M., 1988. Les variations de la couverture forestière mésophile d'Afrique
988 occidentale au cours de l'Holocène. Comptes rendus de l'Académie des sciences. 307(4),
989 439-445.

990 Lézine, A.-M., 1989. Late Quaternary vegetation and climate of the Sahel. Quaternary
991 Research. 32, 317-334.

992 Lézine, A.-M., Duplessy, J.-C., Cazet, J.-P., 2005. West African monsoon variability during
993 the last deglaciation and the Holocene: Evidence from fresh water algae, pollen and isotope
994 data from core KW31, Gulf of Guinea. Palaeogeography, Palaeoclimatology, Palaeoecology.
995 219, 225-237. <https://doi.org/10.1016/j.palaeo.2004.12.027>

996 Lézine, A.-M., Hély, C., Grenier, C., Braconnot, P., Krinner, G., 2011. Sahara and Sahel
997 vulnerability to climate changes, lessons from Holocene hydrological data. Quaternary
998 Science Reviews. 30, 3001-3012. <https://doi.org/10.1016/j.quascirev.2011.07.006>

999 Macklin, M.G., Toonen, W.H., Woodward, J.C., Williams, M.A., Flaux, C., Marriner, N., Nicoll,
1000 K., Verstraeten, G., Welsby, D., 2015. A new model of river dynamics, hydroclimatic change
1001 and human settlement in the Nile Valley derived from meta-analysis of the Holocene fluvial
1002 archive. Quaternary Science Reviews. 130, 109-123.
1003 <https://doi.org/10.1016/j.quascirev.2015.09.024>

1004 Maley J., 1981. Etudes palynologiques dans le bassin du Tchad et paléoclimatologie de
1005 l'Afrique nord-tropicale de 30 000 ans à l'époque actuelle. Ph.D. Thesis, University of
1006 Montpellier, France.

1007 Maley, J., 2010. Climate and palaeoenvironment evolution in North Tropical Africa from the
1008 end of the Tertiary to the Upper Quaternary. Palaeoecology of Africa. 30, 227-278.

1009 Maley, J., Vernet, R., 2015. Populations and climatic evolution in north tropical Africa from
1010 the end of the neolithic to the dawn of the modern era. African Archaeological Review, 32 (2),
1011 179-232. <https://doi.org/10.1007/s10437-015-9190-y>

1012 Makaske, B., 1998. Anastomosing river: forms processes and sediments, Nederlandse
1013 geografische Studies 249, Konnonklijk Nederlands Aadrijksundig Genoostchop. Faculteit
1014 Ruimteelelijke Wetenschappen Universiteit Utrecht, 237 p.

1015 Makaske, B., De Vries, E., Tainter, J.A., McIntosh, R.J., 2007. Aeolian and fluviolacustrine
1016 landforms and prehistoric human occupation on a tectonically influenced floodplain margin,
1017 the Méma, central Mali. Netherlands Journal of Geosciences. 86, 241-256.

1018 Mayewski, P.A., Rohling, E.E., Stager, J.C., Karlen, W., Maash, K.A., Meeker, L.D.,
1019 Meyerson, E.A., Gasse, F., Van Kreveld, S., Holmgren, K., Thorp, J.L., Rosqvist, G., Rack,
1020 F., Staubwasser, M., Schneider, R.R., Steig, E.J., 2004. Holocene climate variability.
1021 Quaternary Research. 62, 243-255. <https://doi.org/10.1016/j.yqres.2004.07.001>

1022 Mayor, A., 2011. Traditions céramiques dans la boucle du Niger : ethnoarchéologie et
1023 histoire du peuplement au temps des empires précoloniaux. Journal of African archaeology
1024 monograph series 7. Peuplement humain et Paléoenvironnement en Afrique de l'Ouest, 2,
1025 Africa Magna Verlag, Frankfurt.

1026 Mayor, A., Huysecom, E., Gallay, A., Rasse, M., Ballouche, A., 2005. Population dynamics
1027 and paleoclimate over the past 3000 years in the Dogon Country, Mali. Journal of
1028 anthropological archaeology. 24, 25-61. <https://doi.org/10.1016/j.jaa.2004.08.003>

1029 Mayor, A., Huysecom, E., Ozainne, S. Magnavita, S., 2014. Early social complexity in the
1030 ogon Country (Mali) as evidenced by a new chronology of funerary practices. Journal of
1031 anthropological archaeology. 34, 17-41. <https://doi.org/10.1016/j.jaa.2013.12.002>

1032 McGee, D., deMenocal, P.B., Winckler, G., Stuut, J.B.W., Bradtmiller, L.I., 2013. The
1033 magnitude, timing and abruptness of changes in North African dust deposition over the last
1034 20,000 yr. Earth and Planetary Science Letters, 371–372, 163–176.
1035 <https://doi.org/10.1016/j.epsl.2013.03.054>

1036 McIntosh, R.J., 1983. Floodplain geomorphology and human occupation of the upper inland
1037 delta of the Niger. Geographical Journal, 182-201.

1038 McIntosh, R.J., 1998. The Peoples of the Middle Niger: The Island of Gold. Blackwell,
1039 Oxford.

1040 McIntosh, R.J., 2005. Ancient Middle Niger. Urbanism and the self-organizing landscape.
1041 Cambridge University Press, Cambridge.

1042 McIntosh, S. K., 1999. Floodplains and the development of complex society: comparative
1043 perspectives from the West African semi-arid tropics. In: Bacus, E.A., Lucero, L.J. (Eds.),
1044 Complex Polities in the ancient Tropical World. American Anthropological Association,
1045 Arlington, pp. 151-165.

1046 McIntosh, S.K., McIntosh, R.J., 1980. Prehistoric investigations at Jenne, Mali: a study in the
1047 development of urbanism in the Sahel. British Archaeology Reports, International Series, 89
1048 (1-2) & Cambridge Monographs in African archaeology, 2. Oxford. (541 p)

1049 McIntosh, S. K., McIntosh, R. J., 1983. Current directions in West African prehistory. Annual
1050 Review of Anthropology. 12 (1), 215-258.
1051 <https://doi.org/10.1146/annurev.an.12.100183.001243>

1052 Miall, A.D., 1996. The geology of fluvial deposits: sedimentary facies, basin analysis and
1053 petroleum geology. Springer, Berlin.

1054 Neumann, K., Kahlheber, S., Uebel, D., 1998. Remains of woody plants from Saouga, a
1055 medieval west African village. Vegetation History and Archaeobotany. 7 (2), 57-77.

1056 Neumann, K., Fahmy, A., Lespez, L., Ballouche, A., Huysecom, E., 2009. The Early
1057 Holocene palaeoenvironment of Ounjougou (Mali): phytoliths in a multiproxy context.
1058 Palaeogeography, Palaeoclimatology, Palaeoecology. 276, 87-106.
1059 <https://doi.org/10.1016/j.palaeo.2009.03.001>

1060 Ngomanda, A., Neumann, K., Schweizer, A., Maley, J., 2009. Seasonality change and the
1061 third millennium BP rainforest crisis in southern Cameroon (Central Africa). Quaternary
1062 Research. 71(3), 307-318. <https://doi.org/10.1016/j.yqres.2008.12.002>

1063 Niedermeyer, E.M., Schefuß, E., Sessions, A.L., Mulitza, S., Mollenhauer, G., Schulz, M.,
1064 Wefer, G., 2010. Orbital-and millennial-scale changes in the hydrologic cycle and vegetation
1065 in the western African Sahel: insights from individual plant wax δD and $\delta^{13} C$. Quaternary
1066 Science Reviews. 29 (23), 2996-3005. <https://doi.org/10.1016/j.quascirev.2010.06.039>

1067 Nizou, J., Hanebuth, T.J.J., Heslop, D., Schwenk, T., Palamenghi, L., Stuut, J. B., Henrich,
1068 R., 2010. The Senegal River mud belt: A high-resolution archive of paleoclimatic change and
1069 coastal evolution. *Marine Geology*. 278, 150 –164.
1070 <https://doi.org/10.1016/j.margeo.2010.10.002>

1071 Notebaert, B., Verstraeten, G., 2010. Sensitivity of West and Central European river systems
1072 to environmental changes during the Holocene: A review. *Earth-Science Reviews*. 103 (3),
1073 163-182. <https://doi.org/10.1016/j.earscirev.2010.09.009>

1074 Ozainne, S., 2013. Un Néolithique Ouest-Africain: cadre chrono-culturel, économique et
1075 environnemental de l'Holocène récent en Pays dogon (Mali). *Journal of African archaeology*
1076 monograph series 8. Peuplement humain et Paléoenvironnement en Afrique de l'Ouest 3,
1077 Africa Magna Verlag, Frankfurt.

1078 Ozainne, S., Lespez, L., Garnier, A., Ballouche, A., Neumann, K., Pays, O., Huysecom, E.,
1079 2014. A question of timing: spatio-temporal structure and mechanisms of early agriculture
1080 expansion in West Africa. *Journal of Archaeological Science*, 50, 359-368.
1081 <https://doi.org/10.1016/j.jas.2014.07.025>

1082 Ozainne, S., Lespez, L., Le Drezen, Y., Eichhorn, B., Neumann, K., Huysecom, E., 2009.
1083 Developing a chronology integrating archaeological and environmental data from different
1084 contexts: the Late Holocene sequence of Ounjougou (Mali). In: Hajdas, I., Della Casa, P.,
1085 Egli, M., Hügi, V., van Willigen, S., Wörle, M. (Eds.), *Proceedings of the 5th International*
1086 *Symposium on Radiocarbon and Archaeology*. *Radiocarbon*. 51 (2), pp. 457-470.
1087 <https://doi.org/10.1017/S0033822200055855>

1088 Passega, R., 1964. Grain size representation by CM patterns as a geologic tool. *Journal of*
1089 *Sedimentary Research*. 34 (4), 830-847.

1090 Passega, R., 1957. Texture as characteristics of clastic deposition, *Bulletin of the American*
1091 *Association of Petroleum geologists* 41 (94), 1952-1984.

1092 Pettitt A.N. 1979, A non-parametric approach to the change-point problem. *Applied statistics*,
1093 vol. 28, n°2, p. 126–135.

1094 Rasse, M., Ballouche, A., Huysecom, E., Tribolo, C., Ozainne, S., Le Drézen, Y., Stokes, S.,
1095 Neumann, K., 2006, Évolution géomorphologique, enregistrements sédimentaires et
1096 dynamiques paléoenvironnementales holocènes à Ounjougou (Plateau Dogon, Mali, Afrique
1097 de l'Ouest). *Quaternaire*. 17, 61-74. <https://doi.org/10.4000/quaternaire.677>
1098 Rasse, M., Soriano, S., Tribolo, C., Stokes, S., Huysecom, E., 2004. La séquence
1099 Pléistocène supérieur d'Ounjougou (Pays dogon, Mali, Afrique de l'Ouest) : évolution
1100 géomorphologique, enregistrements sédimentaires et changements culturels. *Quaternaire*.
1101 15 (4), 329-341.
1102 Reichelt, R., Faure, H., Maley, J., 1992. Die Entwicklung des Klimas im randtropischen
1103 Sahara-Sahelbereich während des Jungquartärs: ein Beitrag zur angewandten Klimakunde.
1104 *Petermanns Geographischen Mitteilungen*, 136, pp. 69-79.
1105 Reimer, P.J., Bard, E., Bayliss, A., Beck, J.W., Blackwell, P.G., Bronk Ramsey, C., Grootes,
1106 P. M., Guilderson, T. P., Hafliðason, H., Hajdas, I., Hattž, C., Heaton, T.J., Hoffmann, D.L.,
1107 Hogg, A.G., Hughen, K.A., Kaiser, K.F., Kromer, B., Manning, S.W., Niu, M., Reimer, R.W.,
1108 Richards, D.A., Scott, E.M., Southon, J.R., Staff, R.A., Turney, C.S.M., Van der Plicht, J.,
1109 2013. IntCal13 and Marine13 Radiocarbon Age Calibration Curves 0-50,000 Years cal BP.
1110 *Radiocarbon*. 55 (4), 1869-1887. https://doi.org/10.2458/azu_js_rc.55.16947
1111 Salzmann, U., Hoelzmann, P., Morczinek, I., 2002. Late Quaternary climate and vegetation of
1112 the Sudanian zone of northeast Nigeria. *Quaternary Research*. 58, 73-83.
1113 <https://doi.org/10.1006/qres.2002.2356>
1114 Schumm, S.A., 1977. *The fluvial system*. Wiley, New-York.
1115 Schumm, S.A., Rea, D. K., 1995. Sediment yield from disturbed earth systems. *Geology*. 23
1116 (5), 391-394. [https://doi.org/10.1130/0091-7613\(1995\)023%3C0391:SYFDES%3E2.3.CO;2](https://doi.org/10.1130/0091-7613(1995)023%3C0391:SYFDES%3E2.3.CO;2)
1117 Schumm, S.A., 1991. *To interpret the Earth. Ten ways to be wrong*. Cambridge University
1118 Press, Cambridge, UK.
1119 Shanahan, T.M., Overpeck, J.T., Wheeler, C.W., Beck, J.W., Pigati, J., Talbot, M.R., Scholz,
1120 C.A., Peck, J., King, J.W., 2006. Paleoclimatic variations in West Africa from a record of late
1121 Pleistocene and Holocene lake level stands of Lake Bosumtwi, Ghana. *Palaeogeography*,

1122 Palaeoclimatology, Palaeoecology. 242 (3-4), 287-302.
1123 <https://doi.org/10.1016/j.palaeo.2006.06.007>

1124 Shanahan, T.M., McKay, N.P., Hughen, K.A., Overpeck, J.T., Otto-Bliesner, B., Heil, C.W.,
1125 Scholz, C.A., King, J.W., Peck, J., 2015. The time-transgressive termination of the African
1126 Humid Period. *Nature Geoscience*. 8 (2), 140-144. <https://doi.org/10.1038/ngeo2329>

1127 Stern, M., Ballouche, A., Weisskopf, E., Landry, D., Laporte, L, in press. Enregistrements
1128 sédimentaires dans la moyenne vallée du Bao Bolon (Sénégal). Première esquisse
1129 chronostratigraphique Holocène. *Quaternaire*.

1130 Stokes, S., Bailey, R.M., Fedoroff, N., O'Marah, K.E., 2004. Optical dating of aeolian
1131 dynamism on the West African Sahelian margin. *Geomorphology*. 59, 281-291.
1132 <https://doi.org/10.1016/j.geomorph.2003.07.021>

1133 Thomas, M.F., 2008. Understanding the impacts of Late Quaternary climate change in
1134 tropical and sub-tropical regions. *Geomorphology*. 101 (1-2), 146-158.
1135 <https://doi.org/10.1016/j.geomorph.2008.05.026>

1136 Trimble, S.W. 1981: Changes in sediment storage in the Coon Creek basin, Driftless area,
1137 Wisconsin, 1853 to 1975. *Science*. 214, 181-83.
1138 <https://doi.org/10.1126/science.214.4517.181>

1139 Valentin, C., Rajot J.L. Mitja, D., 2004. Responses of soil crusting, runoff and erosion to
1140 fallowing in the sub-humid and semi-arid regions of West Africa. *Agriculture, ecosystems and*
1141 *environment*. 104 (2), 287-302. <http://dx.doi.org/10.1016/j.agee.2004.01.035>

1142 Verstraeten, G., Broothaerts, N., Van Loo, M., Notebaert, B., D'Haen, K., Duser, B., De Brue,
1143 H., 2017. Variability in fluvial geomorphic response to anthropogenic disturbance.
1144 *Geomorphology*. 294, 20-39. <https://doi.org/10.1016/j.geomorph.2017.03.027>

1145 Wilcox, A., 1998. Early plant succession on former arable land. *Agriculture, ecosystems and*
1146 *environment*. 69 (2) 143-157. [https://doi.org/10.1016/S0167-8809\(98\)00104-2](https://doi.org/10.1016/S0167-8809(98)00104-2)

1147 Wanner, H., Solomina, O., Grosjean, M., Ritz, S.P., Jetel, M., 2011. Structure and origin of
1148 Holocene cold events. *Quaternary Science Reviews*. 30 (21-22), 3109-3123.
1149 <https://doi.org/10.1016/j.quascirev.2011.07.010>